# Voyager Interstellar Mission

Proposal to Senior Review 2008 of the Mission Operations and Data Analysis Program for the Heliophysics Operating Missions

Edward C. Stone, Project Scientist
John D. Richardson, Proposal Editor
Ed B. Massey, Project Manager

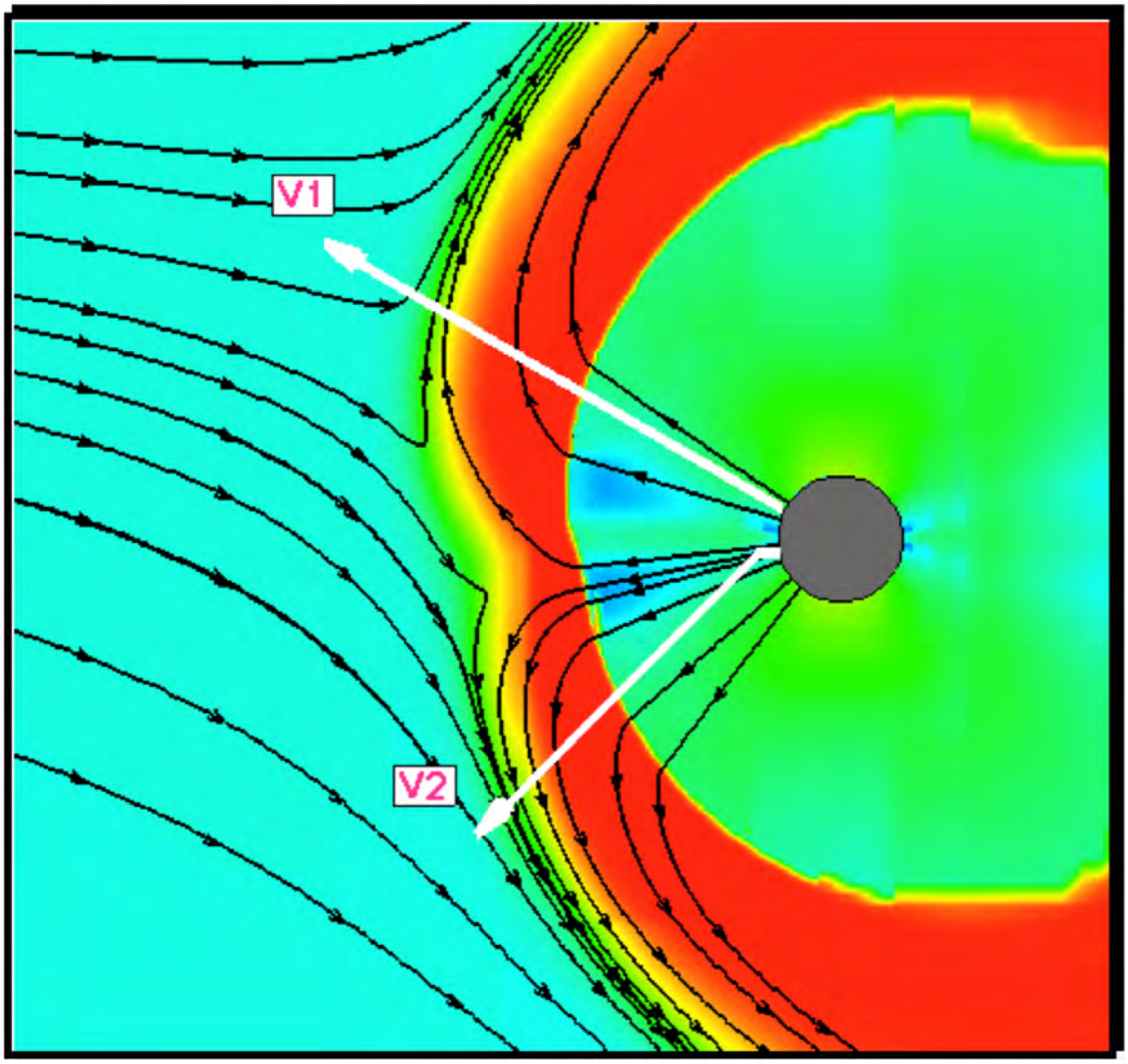


February 2008

## EXECUTIVE SUMMARY

The Voyager Interstellar Mission is exploring the interaction of the heliosphere with the local interstellar medium (LISM). Voyager 1 (V1) crossed the termination shock (TS) of the solar wind in December 2004 and Voyager 2 (V2) crossed it in August 2007. The V2 data provided the first observations of the TS; V1 crossed the TS in a data gap. The Voyager spacecraft are now both taking measurements in the heliosheath (HSH). V2 is making the first plasma observations of the TS region and HSH. We are still assimilating this exciting new data.

The crossings of the TS provided the first concrete information on the scale size and the shape of the heliosphere. Voyager 1, in the northern hemisphere of the heliosphere, crossed the TS at 94 Astronomical Units (AU) while V2, in the southern hemisphere, crossed it at 84 AU. Based on these TS distances and model predictions, the heliopause (HP) and LISM are probably 30-50 AU further out. The asymmetry in the TS crossing distances verifies that the southern hemisphere of the heliosphere is pushed inward, probably by the interstellar magnetic field (ISMF). Although the uncertainties in the HP position are large, the Voyager spacecraft have a good chance of reaching this boundary in their operational lifetimes. With the observed asymmetry both spacecraft may cross the HP at roughly the same time and provide the first direct observations of the LISM.

The V1 and V2 TS crossings provided many surprises that we are still working to understand. V2 crossed the TS at least five times and we have data at three of those crossings. The shock structure observed by V2 showed a very dynamic shock; one crossing had the foot/ramp structure typically observed at quasi-perpendicular supercritical shocks. A second crossing seemed to catch the shock reforming, with two ramp-like structures. We are working to understand these structures. Another TS surprise was that the thermal plasma was heated by a factor of 10-20 less than expected. Models and analogy to planetary magnetospheres suggested the HSH temperature would be 1-2 million degrees K and the electron temperature would be about 30 eV. The observed ion temperature was only about 100,000 K and the upper limit for the electron temperature is 3-4 eV. We think this missing energy went into the pickup ions (PUIs) and are working to model the process. The plasma flow speed is unexpectedly low at V1 and high at V2 and the pickup ions are strongly heated. None of the foregoing observations were anticipated, so these and future revelations of the unexpected nature of the HSH, HP, and LISM will drive theoretical modeling toward a new paradigm.

At the next solar minimum, the Voyagers should be at high enough latitudes to monitor the interaction region between the fast and slow solar wind and to observe coronal hole flow in the HSH. As solar activity increases, we will learn how interplanetary coronal mass ejections (ICMEs) and merged interaction regions (MIRs) propagate through and affect the HSH. We will observe the recovery of cosmic rays beyond 100 AU at solar minimum, determine the effects of a negative magnetic polarity solar cycle, and monitor the unfolding of the low-energy anomalous cosmic ray (ACR) spectra as V1 and V2 move through the HSH.

## 1. INTRODUCTION

The Voyager spacecraft were launched in 1977 on a trajectory toward the giant planets, which serendipitously was also toward the upstream direction of the heliosphere. After the successful planetary encounters, the Voyager Interstellar Mission continued outward with the goal of making the first observations of the LISM. Both Voyagers have now crossed the TS, so the goal of reaching the LISM seems achievable.

The cover figure shows a model of the heliosphere with the plasma flow lines superposed. The color scale shows the magnetic field magnitude. The Voyager trajectories are shown by the white lines. Moving from the Sun outward, we see the solar wind, which becomes supersonic near the Sun and moves at a nearly constant speed radially outward to 80-100 AU, where it encounters the TS and becomes subsonic. The shocked SW in the inner HSH region extends outward to the HP. At the HP boundary, as shown by the flow lines in the figure, the LISM plasma flow diverts around the heliosphere and the shocked solar wind rotates to flow toward the heliospheric tail. This subsonic flow of solar plasma is affected by the LISM, which we think is essentially uniform on the relevant $\sim$100 AU spatial scales and decade-long time scales. The LISM has a magnetic field and is flowing relative to the heliosphere. The HP is expected to be several tens of AU beyond the TS. Beyond this boundary may be a bow shock where the incoming LISM plasma undergoes a shock transition. The region between the HP and BS is known as the outer HSH. The model assumes a magnetic field direction at a 45° angle to the LISM flow vector. which produces an asymmetric heliosphere with the TS and HP closer in the south than the north.

The V1 crossing of the TS set the scale for the whole heliospheric system. The missing piece before this crossing was the pressure in the LISM. Knowing the TS boundary distance fixes this parameter. Models predict that the HP is 30-50% more distant than the TS. The V2 crossing of the TS tells us about the asymmetries in the heliosphere; the boundaries in the south are closer to the Sun than those in the north. The Voy-

ager trajectories are shown in Figure 1. Distance in AU is plotted vs. heliolatitude and times are marked on the trajectory traces. Also marked are the locations of the V1 and V2 TS crossings and the V1 and V2 HP crossings based on model results (see section 3.1). The V1 HP crossing is likely to after 2015 and the V2 HP crossing in a similar time frame. The spacecraft will have sufficient power to operate all instruments until 2016; after this time, power-sharing will extend the useful life of the spacecraft beyond 2020. Thus the Voyagers are likely to provide the first in situ measurements of the LISM.

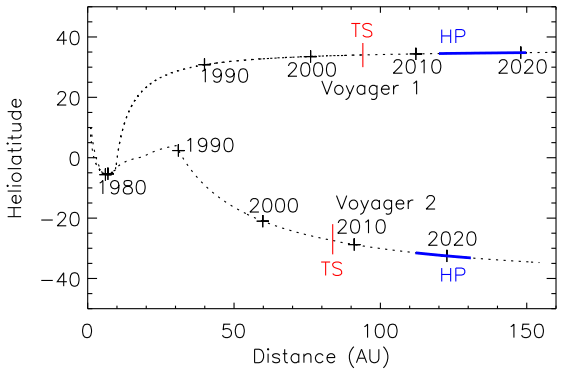


**FIGURE 1.** Trajectories of the Voyager spacecraft.

On their way to the LISM, the Voyager spacecraft are exploring an entirely new region, the HSH. The data show that this region of subsonic flow is very active, with large fluctuations in the plasma and magnetic field over times scales of hours to days. These variations likely result both from structures entrained in the solar wind and from those generated by the motions of the TS and possibly also the HP. Large fluctuations in MeV particle fluxes are observed but not yet understood. This region contributes to the modulation of the galactic cosmic rays (GCRs) [McDonald et al., 2002]. Unanticipated attributes are already being discovered, such as much lower than predicted plasma temperatures, very different plasma speeds at V1 and V2, and an increase of ACR intensities with distance.

The Voyager spacecraft are relatively healthy. The active instrument teams are the Plasma Science experiment (PLS) which measures thermal plasma, the Low Energy Charged Particle experiment (LECP) which detects particles in the tens of keV to tens of MeV range, the Cosmic Ray subsystem (CRS) which measures GCRs and ACRs, the magnetometer experiment (MAG), and the Plasma Wave subsystem (PWS) which observes plasma and radio waves. In addition, the V2 Planetary Radio Astronomy and V1 Ultraviolet Spectrometer instruments still return data, although the science teams are not supported. The V1 PLS experiment failed soon after the Saturn encounter in 1980 and has not been able to detect even the higher plasma fluxes in the HSH, but the V2 PLS experiment is returning excellent data from the HSH. The V2 PWS returns valuable data in many channels and detected emissions at the TS crossing; however, the wideband receiver failed in 2003, the 17.8 Hz channel is intermittent, and the upper 8 channels (1 kHz to 56 kHz) have decreased sensitivity due to a failure in a multiplexor switch in the FDS. The V2 MAG experiment has a continuing problem with noise generated by the spacecraft and other instruments which makes reliable analysis very difficult, but the higher magnetic field strengths in the HSH have made that problem more tractable. Otherwise the instruments work well and all have the sensitivity to continue observations in the environments expected beyond the TS and HP.

The Sun-Solar System Connection (SSSC) Science and Technology Roadmap 2005-2035 sets forth NASA's goals, some of which depend critically upon data from the Voyager spacecraft. The first SSSC objective is to "Understand the fundamental processes of the space environment - from the Sun to Earth, to other planets, and beyond to the interstellar medium". The Voyagers are the only spacecraft positioned to directly observe the boundaries of the heliosphere and have a chance to directly sample the LISM. These boundaries are the largest structures in the heliosphere and allow us to study physical processes such as magnetic reconnection, particle acceleration and transport, and the interaction of the solar wind plasma with the LISM neutrals in a system with scale size ∼100 AU. These three topics, magnetic reconnection, particle acceleration and transport, and plasma-neutral interactions, are priority research focus areas identified by the SSSC roadmap. The unique perspective of the Voyagers is crucial for these studies. In addition, a priority investigation identified in the roadmap, F3.4, is "How do the heliosphere and the interstellar medium interact"? The role of Voyager in answering this question is clearly critical.

The recent scientific discoveries bearing on these roadmap objectives are elaborated on in this proposal. They include the first crossings of the TS, the first observations of the HSH, verification of asymmetries in the heliospheric shape, and the lack of the expected ACR acceleration at the TS.

The Voyagers are the outermost spacecraft in NASA's heliospheric network, the ensemble of spacecraft collecting data in the heliosphere to provide a global picture of heliospheric processes. Voyager plays a critical role, and benefits greatly from, its place in this network. Voyager provides direct observation of ACRs near their source region and of GCRs before they are modulated in the solar wind. Comparison of 1 AU and Ulysses data with Voyager data has provided

tests of models of solar wind evolution. We are now trying to understand how changes in the solar wind propagate through the HSH. Inner heliospheric spacecraft provide data on the solar wind pressure, which controls the motion of the TS. These spacecraft also monitor large solar wind structures such as ICMEs which should cause disturbances in the HSH. Models can be used to determine how the solar wind observed in the inner heliosphere evolves with distance and thus give us a rough idea of the solar wind conditions upstream of the TS. These data will help us understand and differentiate the effects of shock motion and solar wind changes on the HSH. The Voyagers observe the integrated effects of solar wind evolution and interaction with the LISM from the inner to outer heliosphere. The inner heliospheric spacecraft do the reverse, observing the integrated effects of inward motion of ACRs, GCRs, and LISM neutrals from the LISM and TS to 1 AU. These complementary data sets allow us to test models, providing input conditions at one boundary and benchmark observations at the other.

When the Interstellar Boundary Explorer (IBEX) spacecraft joins the heliospheric network in July 2008, the synergy with Voyager data will be even greater. IBEX will measure properties of heliospheric boundaries regions by observing energetic neutral atoms. These observations will provide a global picture of the Sun-LISM interaction at the same time the Voyager spacecraft are exploring the interaction in situ. Voyager directly measures the ions that are the neutral source population which is critical for understanding the IBEX data. The global picture obtained by IBEX will be of great help for understanding the in situ observations and vice versa.

The sections which follow describe five broad science topics being addressed by the Voyager spacecraft. These topics are 1) the TS precursors and the TS crossing, 2) the HSH, 3) energetic particles, 4) cosmic ray modulation, and 5) the HP and interplanetary medium. For each topic we give a description of the science, summarize recent results, and describe how Voyager data will advance our knowledge in these areas in the future.

# 2 TERMINATION SHOCK CHARACTERISTICS

## 2.1 Termination Shock Particles (TSPs)

TSPs are ∼30 keV to a few MeV/nuc ions which are accelerated locally at the TS and/or in the HSH and then escape into the upstream solar wind. V1 began measuring high intensities of >40 keV ions and >350 keV electrons in the solar wind upstream of the TS in July 2002 at a distance of 85.2 AU and a heliographic latitude of 33.8°N [Krimigis et al., 2003; McDonald et al., 2003]. V2 at a heliolatitude of 27.5°S entered the TS foreshock region in Dec. 2004 at 75.2 AU. This difference in location is qualitatively consistent with models which predict both a thicker foreshock region in the direction of V2 and that the TS is closer to the sun in the south than in the north [ Opher et al., 2006; Pogorelov et al., 2006].

Energetic particles enable remote sensing of conditions at the particle source (i.e., the TS and/or the HSH) and in the plasma between the source and the spacecraft. Thus the upstream TSPs can tell us about the global structure of the heliosphere. These important observations include (1) the locations of the particles, (2) their angular distributions, and (3) the spatial and/or temporal evolution of their energy spectra, especially at lower energies. We discuss these points in turn and then possible TSP acceleration processes.

The angular coordinates of the LISM inflow direction are from a heliolatitude of ∼0° and from a heliolongitude ∼3° from the V1 direction and ∼40° from the V2 direction. TSPs measured at V1 in the solar wind from mid-2002 through 2004 were highly anisotropic, beamed mainly away from the sun along the nearly azimuthal spiral interplanetary magnetic field (IMF), rather than toward it as one would expect for a spherical TS. It was soon realized that a TS with a flattened nose could explain these data [Jokipii et al., 2004; Stone, 2004] and that models predict that the TS nose should be flattened [Zank, 1999]. Subsequent model results predicted that V2 should observe TSP anisotropies directed toward the sun, opposite to those observed at V1 [Opher et al., 2006]. Figure 2 shows that anisotropies of the ∼3-17 MeV protons observed at V1 in the foreshock are directed opposite to those at V2, as predicted.

Heliospheric asymmetries may also produce the differences between the energy spectra of 0.04-4.0 MeV TSP ions at V1 and 0.03-3.5 MeV ions at V2. Figure 3 shows foreshock spectra at V1 during 2004.12-2004.81 and at V2 during 2006.64-2007.65 [Decker et al., 2007a]. Intensities at V1 increase monotonically down to at least 40 keV but those at V2 roll over at ∼0.2-0.3 MeV and drop to background below ∼0.1 MeV. More recent data show that the V2 spectrum unrolls slowly as V2 nears the TS, but the lower energies do not increase until V2 is within 30-40 days of its first TS crossing

We do not understand why upstream ion intensities below a few hundred keV are suppressed at V2. Jokipii et al. [2007] suggest that the TS at V2 is more perpendicular than at V1. Lower energy ions would then be unable to propagate into the upstream solar wind as illustrated in Figure 4 (adapted from Giacalone and Jokipii [2006]), which shows V1's path though a quasi-

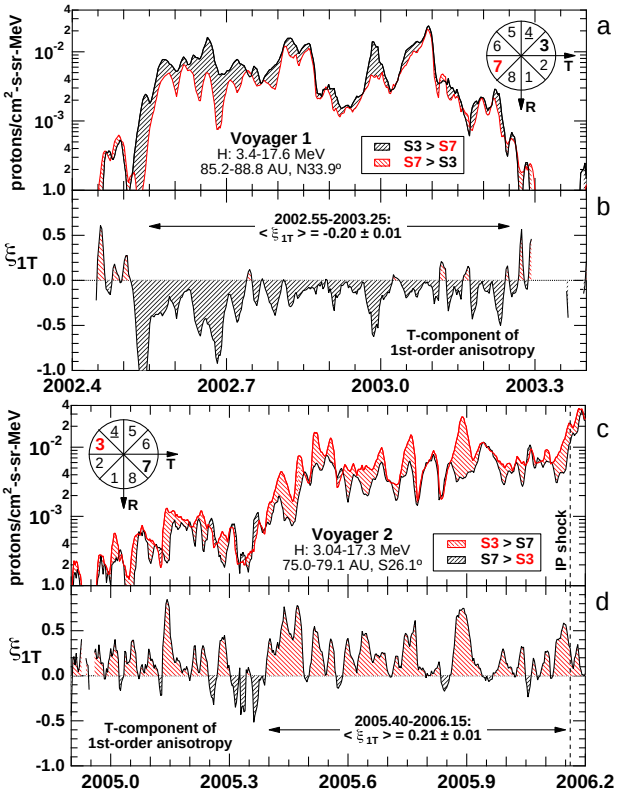


**FIGURE 2.** Daily averages of ∼3-17 MeV protons arriving at V1 (top left) and V2 (top right) from opposite azimuthal directions (see inset pie diagrams), and T-component of 1st-order anisotropy $\xi_{1T}$ (lower panels). Anisotropies at V2 are directed opposite to those at V1, and average values are comparable, with $<\xi_{1T}>$ = -0.20±0.01 at V1 during 2002.55-2003.25, and $<\xi_{1T}>$ = +0.21± 0.01 at V2 during 2005.40-2006.15 [from Decker et al., 2006].

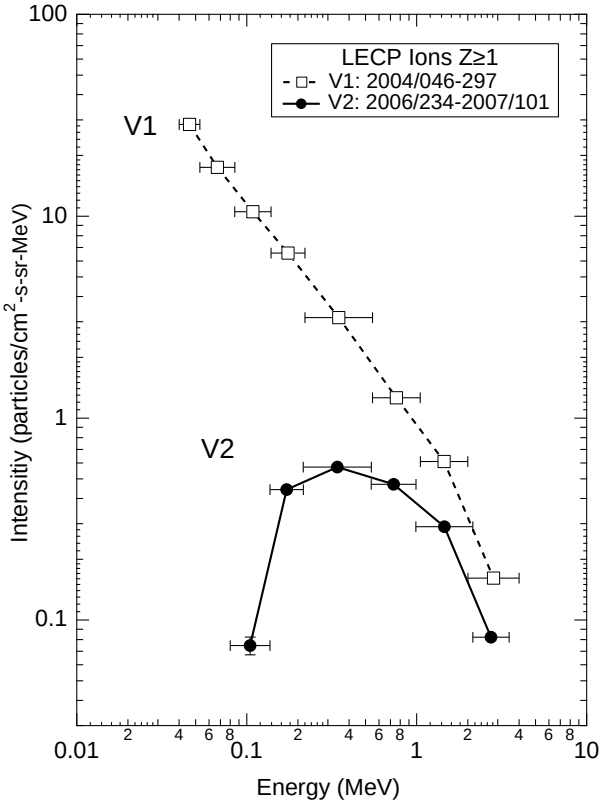


**FIGURE 3.** Comparison of long-term averaged low-energy ion spectra at V1 and V2 in upstream region of TS [from Decker et al., 2007a].

perpendicular TS (thick black line). The mean shock normal **n** is non-radial, so the mean angle $\theta_{Bn}$ between the mean IMF **B** and **n** is ∼80°, enabling lower energy ions to propagate upstream along the meandering IMF. If **n** were more radial at V2, $\theta_{Bn}$ would be closer to ∼90° (thick red line) and upstream escape of lower energy ions would be hindered since these ions would be convected back into the TS. However, this scenario requires that the TS nose be offset by at least 10° from its currently estimated direction [Jokipii et al., 2007]. More work is needed to understand these observations.

The term TSP was adopted initially to differentiate between lower energy ions, <2-4 MeV/nuc, which are accelerated locally at the TS and/or in the HSH and then escape into the upstream solar wind, and the ACR ions with energies >1-300 MeV/nuc which are thought to be accelerated over a broad region of the TS by diffusive shock acceleration (DSA). Section 4 discusses ACRs further. Processes proposed to explain the injection, acceleration, and propagation of TSP ions at the TS include shock surfing [Lipatov and Zank, 1999], inherent fluctuations of $\theta_{Bn}$ [Giacalone, 2005], DSA [Kallenbach et al., 2000] including variations in conditions at the TS [Kota and Jokipii, 2006; Jokipii, 2006; Florinski and Zank, 2006], solutions of the focused transport equation at the TS to treat large anisotropies [Chalov, 2006; leRoux et al., 2007], test-particle TS acceleration and propagation in the fluctuating IMF [Giacalone and Jokipii, 2006]; see also Figure 3], and pickup ion distributions that are pre-accelerated by solar wind turbulence [Fisk and Gloeckler, 2006], heated across the TS [ Fisk et al., 2006], and released into the solar wind [ Gloeckler and Fisk, 2006].

Fisk et al [2006] suggest that solar wind pickup proton distributions with the frequently observed $f(v)\sim v^{-5}$ or $j(E)\sim E^{-1.5}$ tails behave as an ideal gas upon passing through the TS. The HSH pickup proton tail increases in intensity but its spectral form is maintained (Figure 5), which provides an explanation for the ∼-1.5 spectral index of the 0.04 to 2 MeV ions observed in the HSH [Decker et al., 2005]. The V2 0.03-3.5 MeV ion energy spectra in the HSH are harder than

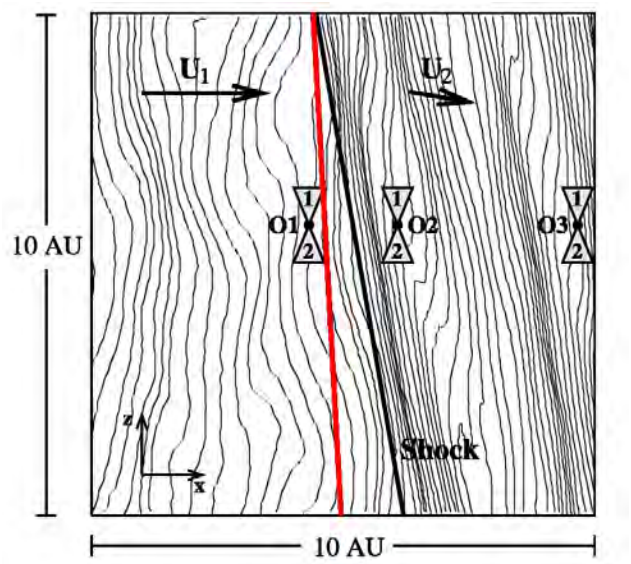


**FIGURE 4.** Schematic illustration of a possible path of V1 through the TS (thick black line) which shows a radial solar wind flow with a meandering, but on average Parker spiral, IMF incident on a TS with non-radial normal. At the TS with a more nearly radial normal (thick red line), the possible case at V2, the TS surface would be more nearly parallel to the mean IMF and low-energy ions would not be able to escape upstream [adapted from original figure in Giacalone and Jokipii, 2006].

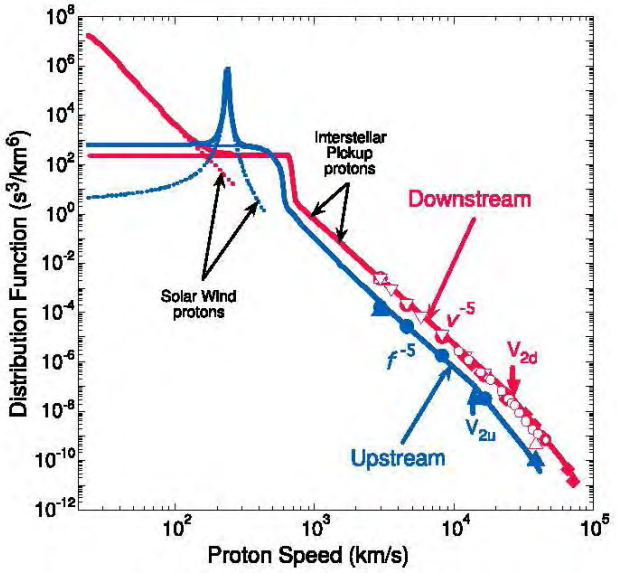


**FIGURE 5.** Phase space density vs. proton speed upstream and downstream of the TS. Sums of the solar wind and pickup proton model spectra are shown as thick curves (upstream in blue and downstream in red). Thin curves indicate upstream (blue) and downstream (red ) pickup proton (solid ) and solar wind proton (dotted ) model distributions. Blue (upstream to TS) and red (downstream from TS) symbols indicate V1 measurements: filled circles are LECP 26-day average spectra, triangles are LECP 20-day average spectra, inverted triangles are LECP 170-day average downstream spectrum, diamonds are 160-day average downstream spectrum, and circles are CRS 1-day average spectrum 68 days after TS crossing. LECP ion differential intensities are divided by 1.5 to remove contributions from ions heavier than protons. In the phase space vs. speed representation the V1 spectra are power laws with spectral index $\gamma$=-5 both upstream and downstream of the TS [From Fisk et al., 2006].

those at V1. However, V2 is still relatively close to the TS and the ion intensities are highly variable. When V2 penetrates deeper into the HSH we will measure quasi-stationary spectra which we can compare with the Fisk et al. [2006] predictions. We also need to carefully examine upstream intensities at V2 for evidence of a pre-accelerated pickup proton seed population.

## 2.2 TS Structure: Initial V2 Results

**Upstream effects**. V2 first crossed the TS in a data gap on day 242 of 2007. The TS then moved outward past V2 on day 243. V2 remained in the solar wind for about 3.5 hours, then the shock moved inward past V2. Three hours later another crossing occurred just before a data gap; since the end of day 244, V2 has remained in the HSH.

The first solar wind signature of the TS was probably the speed decrease on day 160, 82 days (0.8 AU) before the TS crossing. A second speed decrease occurred on day 192 and a third on day 230. Figure 6 shows the energy/proton, which decreases as the speed decreases. The solar wind speed decreased from 400 to 300 km/s before the TS crossing, so almost half of the solar wind flow energy is removed and presumably transferred to energetic particles and/or pickup ions upstream of the TS. We need to quantify and understand this process.

One hypothesis is that the flow energy heats the TSP ions. The first 2 of the step-like energy decreases before the TS were associated with MIRs identified in Figure 6 by the strong fields. We are investigating whether these MIRs trap particles between the TS and the MIR where they undergo Fermi acceleration, with the energy coming from the bulk motion of the solar wind.

Another hypothesis proposed for the pre-shock solar wind slowdown is that hot electrons in the TS foreshock greatly increase the ionization rate of neutral interstellar hydrogen and that acceleration of these pickup ions slows the solar wind. V2 and Ulysses plasma measurements established that the solar wind slows down gradually because of mass loading from pickup ions created by charge exchange and photo-

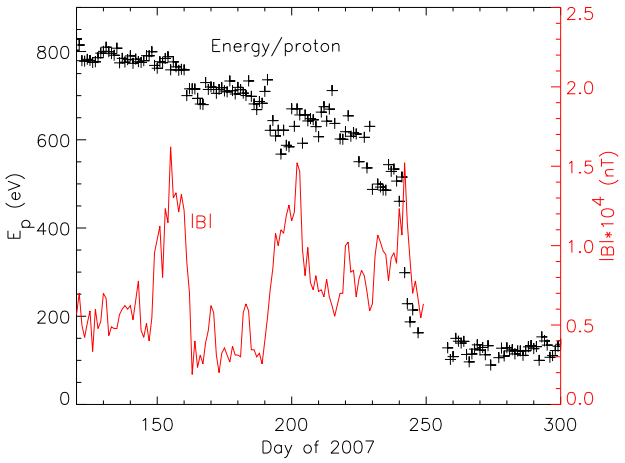


**FIGURE 6.** Total energy/proton (flow energy plus thermal energy) at V2 near the TS. The magnitude of B is shown in red.

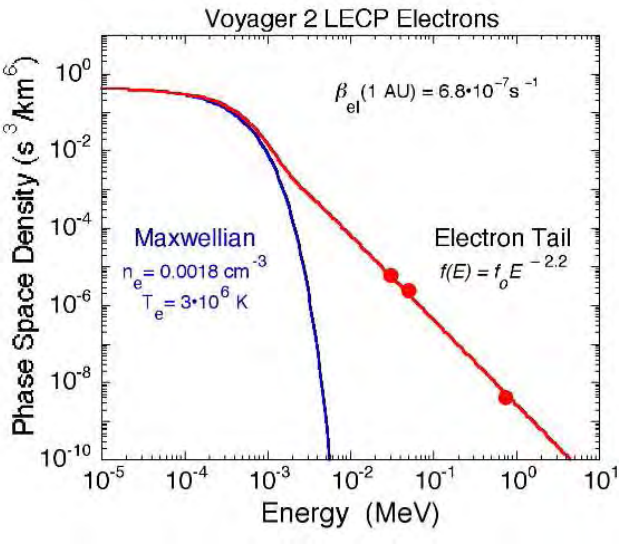


**FIGURE 7.** Electron spectrum in the HSH that will ionize neutral hydrogen at a rate required to produce the observed rapid slow down of the solar wind. Solid circles are V2 LECP electron measurements [provided by G. Gloeckler].

ionization of neutral interstellar hydrogen [Richardson et al., 2008]. To reproduce the observed slowdown in front of the TS would require a relatively large H ionization rate, $\sim 6.5\times10^{-7}$/s just upstream of the TS, that falls off exponentially with an e-folding distance of ∼0.25 AU upstream of the TS. This large electron impact ionization rate would require an electron spectrum upstream of the TS similar to the one shown in Figure 7. The high-energy power law tail of the spectrum is well measured by both V1 and V2. For the low-energy portion, below a few hundred eV, a Maxwellian with density 0.0018/cm$^{-3}$ and temperature of $3\times10^6$ K was assumed. Electrons with energies from ∼40 to ∼400 eV contribute most to the ionization cross section. Observations of electrons in the HSH, especially at energies below a few keV, are important to validate this scenario for the rapid solar wind slowdown. Long integration times may be required to accomplish this.

**The Termination Shock**. Prior to the V1 crossing of the TS, the TS was generally assumed to be a strong perpendicular shock with a magnetic field and density increase of a factor of 4 at the shock. The strength of the TS at V1 could only be estimated since the crossing occurred during a data gap. Measurements showed a magnetic field increase of a factor of betweeen 2 and 3.5, depending on the averaging interval used [Burlaga et al., 2006a]. Measurements of the energetic particles on V1 suggest the shock strength was $2.6^{+0.4}_{-0.2}$. Thus, the TS crossed by V1 was weaker than expected.

V2 crossed the TS at least five times; detailed plasma and magnetic field observations were transmitted for three of these crossings. The multiple crossings indicate that the TS is dynamic, moving in response to fluctuations in the solar wind and/or waves propagating on the shock. The magnetic field observations found that the TS was a perpendicular shock, as expected. Preliminary measurements from both the plasma and magnetic field instruments indicate a shock strength of $B_2/B_1 \sim N_2/N_1 \sim 2.0$, confirming that the strength of the TS is moderate.

Across the TS the solar wind speed drops by a factor of about 2 and the density and magnetic field magnitude rise by a similar factor (thus the shock strength of two). The thermal speed of the protons increases from about 10 to 50 km/s, a factor of 16 in temperature, to $\sim10^5$ K, significantly lower than the $\sim10^6$ K expected. The bulk speed remains above the fast mode speed in the HSH; this result was unexpected and models for the TS including pickup ions are being developed. Figure 6 shows that the HSH plasma has only about 20% of the pre-shock solar wind energy. The remaining energy must be transmitted to some other component of the HSH, possibly the pickup protons or other particles and waves. Energy partition at the TS will be a major topic of investigation during the next few years.

The V2 observations at the three TS crossings show that the structure of the TS is dynamic, changing and possibly reforming on a scale of a few hours. Figure 8 shows a TS crossing which looks like a classical supercritical perpendicular shock, with a foot, ramp, overshoot, undershoot, and damped oscillations. The density showed a large increase after the second TS crossing coincident with a temperature increase; this feature and other small scale structures are not yet

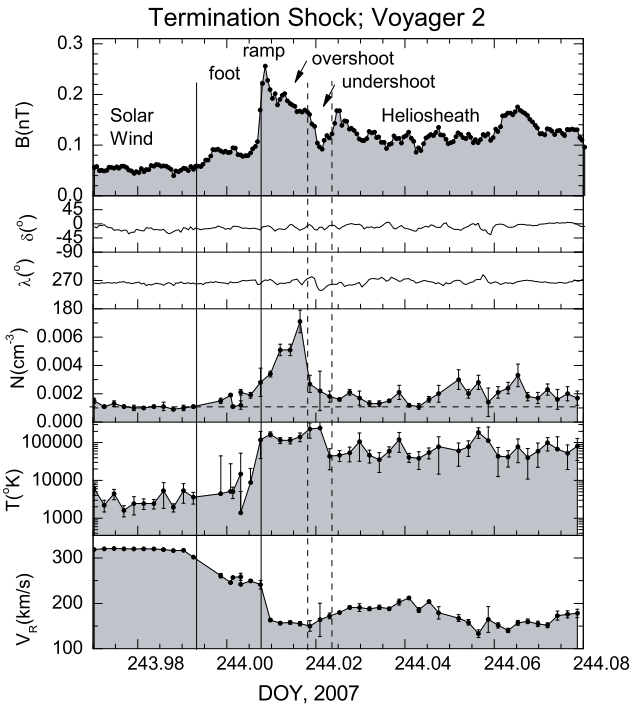


**FIGURE 8.** A V2 TS crossing on day 244 showing a classical supercritical perpendicular shock, with a foot, ramp, overshoot, undershoot, and damped oscillations.

understood. The next TS crossing a few hours later showed some of the same features in a modified form, indicating an evolving structure. The first of the 3 observed TS crossings showed a gradual increase in the plasma flow speed and had a complex magnetic field structure, not resembling the simple supercritical shock, but consistent with the predictions of hybrid and full particle codes that such a shock is nonstationary and undergoes reformation on time scales of order of the ion Larmor period. A better theoretical understanding of the effects of pickup protons and energetic particles on the structure of the TS is needed. These results will be strongly constrained by further analysis of the observations. A basic understanding of the internal structure of the TS should be obtained in the next few years.

**Plasma Waves**. As predicted, and as at V1 [Gurnett and Kurth, 2005], V2 observed Langmuir waves upstream of the TS. V2 observed intermittent upstream waves for only about a month prior to the TS crossing whereas V1 observed these waves for ∼9 months. This difference may indicate that V1 made several close approaches to the TS before the actual crossing. V2 also observed broadband bursts of electrostatic noise, signatures of a shock crossing, near times when the plasma instrument observed evidence of shock-like changes in the solar wind velocity, density, and temperature. The TS wave spectrum is similar to that of other shocks in the heliosphere, such as planetary bow shocks and interplanetary shocks. V2 did not observe the TS-associated electron beams responsible for Langmuir wave generation. However, LECP does observe an energy-dependent ion anisotropy with only ≥200 keV ions moving in the upstream direction. If these >200 keV ions can escape the TS, electrons with similar speeds (≥100 eV energies) may also escape and produce a bump-on-tail in the electron distribution near 100 eV. In future work these preliminary results will be analyzed in detail and the plasma physics of wave generation given careful theoretical attention.

## 2.3 Prospects for More TS Crossings

In addition to the multiple TS crossings due to relatively short-term variations, can we expect more TS crossings on a long-term basis? The variation in the TS distance is caused mainly by changes in the solar wind dynamic pressure. The solar wind dynamic pressure varies over a solar cycle; the variation seems to be the same at all heliolatitudes [Richardson and Wang, 1999]. The solar wind dynamic pressure increases by a factor of ∼2 over a 1-2 year period just after solar maximum, then decreases slowly over the next 9-10 years before increasing again. Recent Wind data from 1 AU show that the solar wind pressure decreases over the past year; this pressure reduction is now reaching the TS and it should move inward. We thus expect the TS to keep moving inward over the next 4-5 year. Our best hope for another TS crossing is for a large transient ICME in the next year to drive the TS outward or for the TS to rebound outward as it recovers from previous transient events in the solar wind [Washimi et al., 2007].

## 2.4 Future Tasks

• Study via theory and modeling why evolution of low-energy TSP ion energy spectra in the TS foreshock differ at V1 and V2 and what implications these data have for heliospheric asymmetries.
• Understand why energy spectra of low-energy HSH ions are harder at V2 than at V1 and what this implies for models of PUI pre-acceleration in the SW and acceleration and/or heating at the TS and in the HSH.
• Model the TS including pickup ions to understand energy partition.
• Quantitative analysis of pre-shock slow down of the solar wind and comparison with particle acceleration.
• Detailed analysis of all the shock crossings - derive better estimates of shock speeds.
• The TS may be very dynamic, forming, then dissipat-

ing and reforming upstream. We need to understand how this process works and how the HSH is affected.
• Study the detailed structure of the TS to see if it is a good particle accelerator - in particular, is shock surfing a viable acceleration mechanism at the TS?
• Continue to look for more TS crossings.
• Examine spectral features for signs of multiple-energy-scale acceleration processes or multiple particle sources.
• Study anisotropies as a function of energy and species upstream and downstream of the TS to characterize transport regimes.

## 3. HELIOSHEATH PHYSICS AND STRUCTURE

The inner HSH is the region between the TS and the HP. The in situ exploration of the HSH began when V1 crossed the TS on 16 December, 2004 and will continue until V1 and V2 cross the HP and enter the LISM. The flows and magnetic field in the HSH are strongly affected by: (a) the solar wind, pickup ions and the interplanetary magnetic field in the supersonic solar wind; (b) the neutral H atoms from the LISM; (c) the interstellar magnetic field; and (d) the ionized component of the interstellar medium. The structure of the HSH is expected to vary with the solar cycle, as the consequence of varying solar wind input conditions to the HSH.

### 3.1 Heliosheath Size and Shape

V1, at 34°N, crossed the TS and entered the HSH at 94 AU. V2, at 27°S, entered the HSH at 84 AU. Thus, the region of supersonic solar wind ends and the HSH begins at ∼90 AU near the end of the declining phase of the solar cycle in the upstream direction. The crossing of the TS by V2 was 10 AU closer to the sun than that of V1, consistent with an asymmetry in the shape of the HSH (assuming the effects of transients and solar cycle variations on the position of the TS are small).

Asymmetries in the shape of the HSH (Figure 9) have been predicted. An ISMF oriented obliquely to the interstellar velocity can produce a lateral or north-south asymmetry in the heliospheric shape [Pogorelov and Matsuda, 1998; Ratkiewicz et al., 1998; Pogorelov et al., 2004; Opher et al., 2006]. Using charged particle and radio data, Opher et al. [2006; 2007] found that the direction of the ISMF in the LISM is ∼60° from the flow direction. This ISMF direction results in higher magnetic pressure on the southern hemisphere when the ISMF drapes around the heliosphere, which pushes the heliosphere inward in the south (see Figure 9). The

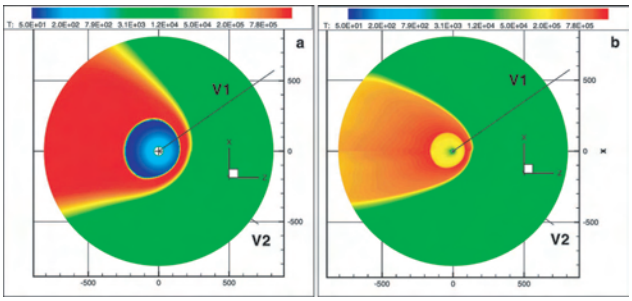


**FIGURE 9.** Plasma temperature distributions in the meridional plane for $B_\infty$ in this plane with a tilt of 45° to the ecliptic, $\beta = 0$, and $B_\infty = 2.5$ $\mu$G. (a) Ideal magnetohydrodynamic (MHD) calculation without an interplanetary B; (b) plasma neutral 2-fluid model with $n_\infty = 0.15$ cm$^{-3}$ and with an interplanetary B. The lines represent the trajectories of V1 and V2. The TS asymmetry is smaller in (b) owing to charge exchange.

Opher et al. [2006] model does not include charge exchange with the interstellar neutrals, which may substantially decrease the magnitude of the asymmetry of the heliosphere caused by the ISMF [Pogorelov et al., 2006; 2007b].

The ISMF also produces an asymmetry in the thickness of the HSH, with a thicker HSH in the north than in the south. The Opher et al. [2006] model predicts that the HSH thickness is about 57 ± 2 AU (39 ± 6 AU) in the V1 (V2) direction. Pogorelov et al. [2004] predict HSH thicknesses (where we scale their numbers to the observed TS crossings) of 30-60 AU. Heerikhuisen et al. [2006a, 2007] include neutrals and predict that the HSH thickness is 70-75 AU (50-55 AU) in the V1 (V2) direction. The width of the HSH is 20% less if one assumes a $\kappa$ distribution function for the solar wind plasma. The value of $\kappa$ =1.63 takes into account the presence of the hot, non-thermal component in the solar wind plasma and agrees with pickup ion (PUI) observations. This $\kappa$ gives a HSH width of about 60 AU (45 AU) in the V1 (V2) direction. We note that these models do not include all the relevant physics, such as the strong heating of pickup ions and the fast flow observed in the HSH, so these results may overestimate the HP distance. V1 and V2 will provide strong constraints on the thickness of the HSH in the north and south, respectively, when they cross the HP.

Asymmetries of the TS and HSH could be introduced or modified by 3-D unsteady phenomena. For example, if a global MIR (GMIR) or another large solar wind disturbance were not spherically symmetric, it could introduce a substantial asymmetry in the TS [Pogorelov and Zank, 2005; Pogorelov et al., 2007b]. Even a spherically symmetric perturbation can increase the TS asymmetry introduced by the ISMF. Washimi et al. [2006; 2007] find that tran-

sients [Richardson et al., 2006; 2007] which propagate through the HSH and interact with the HP influence the position and shape of the TS.

It is important to distinguish between the TS asymmetry inferred from the observations and that obtained in different numerical models. The asymmetry observed by the Voyager spacecraft helps derive important information about the solar wind and LISM properties. Only continued observations by V1 and V2 can determine the relative importance of the ISMF effects, charge exchange, and transient phenomena that control the size and shape of the HSH.

### 3.2 Heliosheath Composition

The LISM surrounding the heliosphere is weakly ionized. The interaction between the LISM and the heliosphere is crucially affected by charge exchange between neutral and charged particles [Wallis, 1975; Baranov and Malama, 1993]. Ulysses observations of pickup ions [Gloeckler et al., 2004] and the slowdown of the solar wind [Richardson et al., 2008] suggest the density of neutral interstellar H at the TS is about 0.1 $cm^{-3}$. Self-consistent MHD-neutral heliospheric models show that for a TS H density of 0.1 $cm^{-3}$ the number density of LISM H $n_\infty$ is $\sim$0.15 $cm^{-3}$ and the number density of LISM $H^+$ is $\sim$0.05 $cm^{-3}$ [Izmodenov et al., 2005, Heerikhuisen et al., 2006a, b; Pogorelov et al., 2007]. Charge exchange influences the flows within both the supersonic solar wind (solar wind) and the outer HSH. The solar wind is decelerated by mass loading of PUI as it moves toward the TS. The PUIs are hot, dominating the internal pressure of the solar wind beyond 20 AU; therefore PUIs strongly influence the solar wind dynamics [Burlaga et al., 1994]. Charge exchange decreases the heliocentric distances of the TS, HP, and BS. In the outer HSH, the LISM protons decelerate when they approach the HP. This deceleration results in a difference between the velocity of protons and neutral H-atoms, leading to enhanced charge exchange which slows down the H and produces a layer of increased H-atom density (a "hydrogen wall") in the outer HSH. The existence of the hydrogen wall is supported by the Lyman-$\alpha$ absorption measurements in directions to different nearby stars [Wood et al., 2004].

### 3.3 Large-scale Flow, Internal Energy, and Magnetic Field in the Heliosheath

The plasma flow velocity as a function of position is a fundamental characteristic of the HSH. In lieu of plasma data from V1, the LECP team used angular data from low-energy ions to estimate the projection of the plasma flow velocity onto the RT-plane [Krimigis et al., 2005; Decker et al., 2005]. Figure 10 shows 26-day averages of the estimated plasma flow speed W = $(W_R^2+W_T^2)$, flow azimuth = $\tan^{-1}(W_T/\ W_T)$, and components $W_R$ and $W_T$ during 2005.5-2007.9 [Decker et al., 2007b]. These results were obtained using the 53-85 keV ion channel. Comparable results are obtained using the 40-53 and 85-139 keV ion channels. The first half of 2005 is not shown since the estimated flows were small and highly variable. Panel (a) shows that W has remained nearly constant, with mean 81 $\pm$ 19 km $s^{-1}$. The large-scale variations, lasting $\sim$0.25 year, may be associated with transient disturbances in the solar wind [Decker et al., 2006]. Although LECP cannot measure the normal velocity component $W_N$, if this component were comparable in magnitude to $W_R$ and $W_T$ ($W_N$ = 50-60 km $s^{-1}$), the flow speed would be 100 km $s^{-1}$ (corresponding to an upstream solar wind speed of 200-400 km $s^{-1}$ for a shock compression ratio of 2 - 4).

Panel (b) of Figure 10 shows that $\lambda$ has been decreasing slowly in magnitude. The flow direction has swung rapidly to a more radial flow at least four times, followed by more gradual returns to previous values. But since at least mid-2006, $\lambda$ has shown a longer-term variation, possibly due to the rotation of the HSH flow velocity toward the plane of the HP as V1 moves outward. The direction of the flow is rotating in the RT-plane from the +R direction toward the -T direction. The correlation coefficient for the fit is r=0.62. The probability of exceeding this r from a fit to 34 uncorrelated data points is <0.001. The linear least-squares fit (dashed diagonal line) shows a change in flow angle of -10°/yr. A linear extrapolation of this result suggests that it will take 9 years for the flow to rotate through 90° at V1, so the HSH thickness along the V1 path would be about 32 AU. V1 would reach the HP in 2013 at about 125 AU. When the fit line in Figure 10 is extrapolated back to the TS crossing, this flow angle is approximately 345°, a 15° departure from radial flow, consistent with the non-radial normal expected at a blunt TS [Giacalone and Jokipii, 2006]. Thus we think we can make good estimates of when the HP will be detected from the V1 ion data. Voyager 2 has a functioning plasma detector and is moving in a different direction, so it will provide data complementary to V1.

Since the magnetic field is frozen-in to the plasma, a rotation of V as V1 (or V2) moves toward the HP implies a corresponding rotation of B. Both the magnetic field and velocity should be parallel to the surface of the HP on average, at the HP [Zank, 1999]. A key issue is where the turning of B and V become evident and how it takes place. Observations by V1 and V2 during the next few years will provide an answer to this question.

The LECP instrument measures eight ion channels that cover the energy ranges 0.040-4.0 MeV and 0.028-

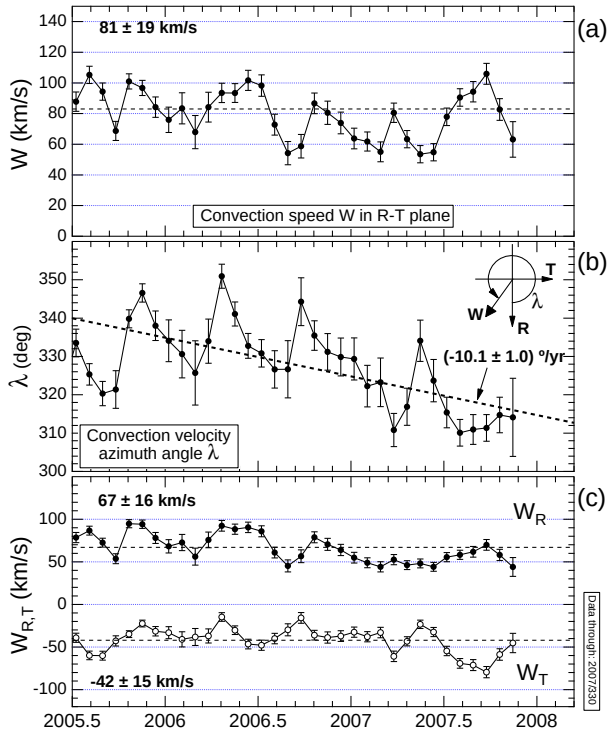


**FIGURE 10.** Estimated RT-component of HSH flow velocity derived from analysis of 26-day averaged angular data of protons 53-85 keV measured by the V1/LECP instrument: (a) Speed W, (b) azimuth $\lambda$, and (c) components $W_R$ and $W_T$. All values are expressed in the sun-fixed inertial frame by correcting for the 17 km $s^{-1}$ spacecraft speed.

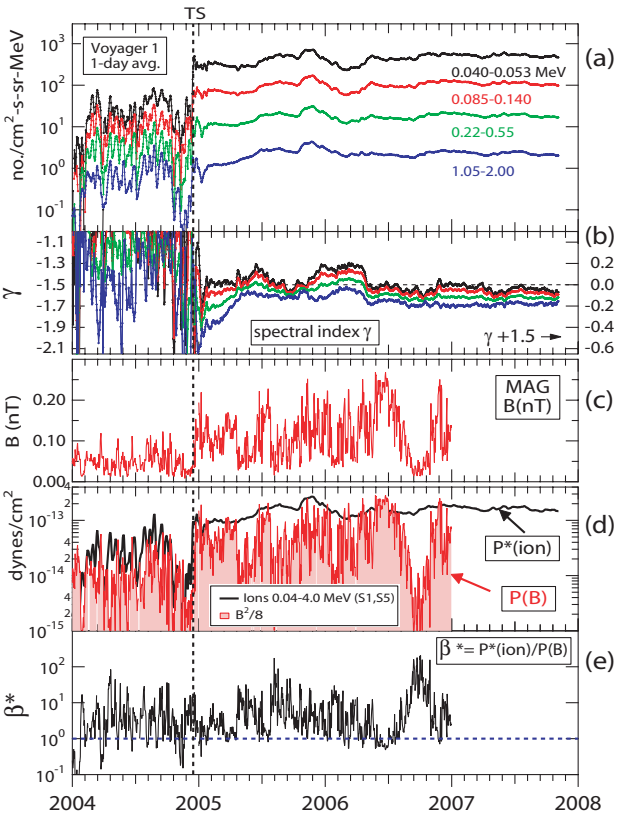


**FIGURE 11.** Comparison of daily-averaged V1/LECP and V1/MAG data during 2004-2007. (a) Low-energy ion (mainly proton) intensities in 4 energy channels. (b) Energy spectral slopes (left axis) and departure of these slopes from -1.5 (right axis) of the intensities in panel (a) evaluated at the logarithmic mean of the channel passband. (c) Magnetic field magnitude. (d) Proton distribution partial pressure P*(ion) in the energy range 0.04-4.0 MeV and magnetic field pressure P(B). (e) Beta calculated as the ratio of the proton partial pressure P*(ion) to P(B).

3.5 MeV on V1 and V2, respectively. Heliosheath ions observed in this energy range are well above thermal proton energies (0.01 keV in a $10^5$ K HSH) and well below the ACR energies (tens of MeV $nuc^{-1}$). These HSH ions include heated and accelerated pickup ions (mostly protons) [Decker et al., 2005; Fisk et al., 2006] which contribute to the suprathermal tail of the HSH proton distribution.

Figure 11 compares the daily averages of low-energy ion intensities measured by V1 with the magnetic field magnitude B during 2004-2007. The TS crossing marks a transition of the ion intensities. In the solar wind, the intensities vary rapidly and are highly anisotropic; in the HSH the intensities are relatively steady and featureless, with greatly reduced anisotropies [Decker et al., 2005; 2006]. The magnetic field strength B increases across the TS, but it varies greatly over a range of time scales [Burlaga et al., 2005b].

Figure 11, panel (d), shows magnetic field pressure $P(B) = B^2/8\pi$ and proton partial pressure P*(ion) calculated using ion intensities in the sunward and anti-sunward viewing sectors of the LECP instrument, which are on average transverse to B. In the HSH, P*(ion) is relatively featureless and flat with mean 1.5 x $10^{-13}$ dynes $cm^{-1}$, while P(B) is variable and often much less than P*(ion). Panel (e) shows that the proton partial beta $\beta^* = P^*(ion)/P(B)$ is large during 2006.6-2006.9 when V1 is deep within the HSH. Continued observations by V1 and the new HSH data from V2, which include plasma data, should provide a better understanding of the distribution of internal energy in the HSH as a function of distance.

As the shocked solar wind slows down in the HSH, the azimuthal component of the magnetic field increases, particularly in the direction of the nose of the HP where the velocity goes to zero [Parker, 1962]. The increasing B will drive an azimuthal flow (the Axford-Cranfill effect). The magnitude of the compression in

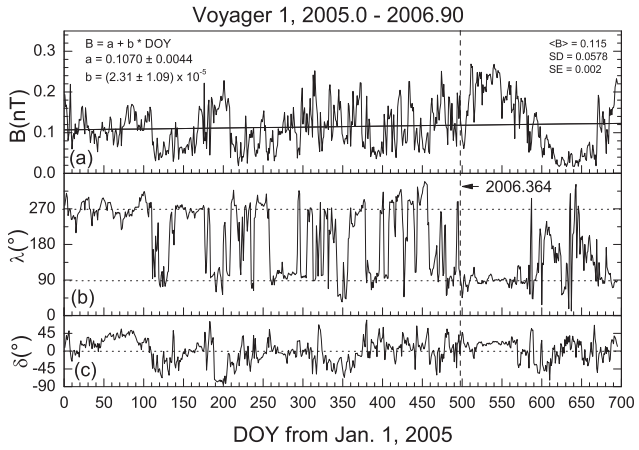


**FIGURE 12.** Daily averages of the magnetic field strength B, azimuthal angle $\lambda$, and elevation angle $\delta$ during 2005 and 2006. The dashed line in Figure 12 is the time at which the HCS dropped below the latitude of V1 as activity declined.

B and of the induced flow speed are not known. Figure 12 shows that at V1 B increased little, if at all, with distance during 2005 and 2006 [Burlaga et al., 2007a]. Further observations are needed to determine and understand the large-scale variation of B in the HSH.

The 3-D MHD simulations of Linde et al. [1998] and Opher et al. [2003; 2004] predict the presence of magnetic ridges beyond the TS, deep in the HSH. If these models were correct, the magnetic field would become increasingly important to the dynamics of the flow. The V1 and V2 measurements of the magnetic field will allow us to determine whether a magnetic ridge is present and if it is caused by deceleration of the HSH flow.

The heliospheric current sheet (HCS) is a fundamental feature of the supersonic solar wind. A major question concerns the behavior of the HCS and the associated magnetic sectors beyond the TS. In analytic studies, Nerney et al. [1995] predict a complex interaction in the HSH due to solar cycle effects with quasi-periodic regions of opposite magnetic polarity of width ∼0.2 AU. They suggest that reconnection might play a major role in this region, as magnetic fields of one sector in the HCS are pressed against the ISMF draped around the HP. Their studies, however, were made in the kinematic approximation where the magnetic field reaction on the flow was neglected.

The sector structure in the HSH was observed by V1 [Burlaga et al., 2005a; 2006a] and is more complex than assumed in the early theoretical studies. This result is not surprising, because the sector structure in the distant supersonic solar wind is much less ordered than at 1 AU due to dynamical interactions which occur beyond ∼10 AU. A better understanding of the sector structure in the HSH and its variation with the solar cycle will be obtained with further observations by V1 and V2.

Evidence for possible reconnection at a sector boundary in the HSH was reported [Burlaga et al. 2006b], but it was highly localized and does not appear to alter the global topology of the magnetic field. Reconnection is not observed at every crossing of the HCS. The role of reconnection in the more distant HSH is unknown, but will be determined by continued Voyager observations.

Among the global MHD modeling efforts to characterize the interaction of the solar system and the interstellar medium, very few include both the solar magnetic field and the ISMF [Linde et al., 1998; Pogorelov et al., 2004, 2006, 2007; Heerikhuisen et al., 2007; Washimi and Tanaka, 1996; Opher et al., 2006, 2007; Washimi et al., 2007]. The models vary between purely MHD, multi-fluid and a combination of MHD and kinetic treatment for the neutral H atoms. All these models, however, assume a HCS parallel to the solar equatorial plane. The inclusion of a tilted and warped HCS sheet in global MHD simulations is a challenging task since high spatial resolution is needed to be able to capture the HCS oscillation.

It is not clear whether the HCS substantially modifies the flows in the HSH, although some studies have proposed such effects. For example, Opher et al. [2003, 2004] suggest the possibility of instabilities near the HCS, with a narrow jet of high-speed flow, strong warping of the HCS, and movement of the HCS away from the ecliptic. The instability has a characteristic wavelength of tens of AU. Thus the region near the current sheet in the HCS might be unstable and dynamic on the scale of the HCS. Such instabilities could produce high levels of turbulence, back flows, and gradients of density and pressure. No evidence for this instability has been found in the V1 data, but instabilities may develop farther out in the HSH. The plasma observations from V2, combined with the observations of B, will determine the extent to which the HCS is a dynamical structure that modifies the global structure of the HSH.

The H flow direction at distances of about 10 AU from the Sun, observed by the SOHO SWAN experiment, is $4^\circ \pm 1^\circ$ from the direction of the He flow (which coincides with the H-atom velocity direction in the unperturbed LISM) [Lallement et al. 2005]. Lallement et al. [2005] suggest that the deflection could be caused by the ISMF pressure if the ISMF is at an angle of $\sim 45^\circ$ to the LISM velocity. This angle was determined using the MHD-neutral calculations of Izmodenov et al. [2005], which did not include the IMF. If the IMF were taken into account, the deflection would take place not only in the B-V plane but also, to a lesser extent, perpendicular to it [Pogorelov and Zank, 2006; Pogorelov et al., 2007]. Such calculations are

important for understanding the source location of the 2-3 kHz radio emission observed by Voyager [Opher et al., 2007; Pogorelov et al., 2007]. Since the radio emission is associated with GMIRs, there is a need for MHD-neutral calculations to model a GMIR propagating through the heliosphere, similar to those of Pogorelov and Zank [2005].

### 3.4 Solar Cycle Variations

Models of the HSH thickness suggest that the Voyager spacecraft will spend the better part of a solar cycle in the HSH and will be able to study the time evolution of the HSH. In situ observations at 1 AU during 2007 show the presence of corotating streams. The minimum of solar cycle 23 ended with the start of cycle 24 in early January, 2008 [NOAA]. At solar minima, solar activity is low, so the heliosphere is less disturbed by coronal mass ejections (CMEs) and the MIRs they produce beyond several AU. The solar wind takes roughly one year to propagate from the Sun to the Voyager spacecraft. Thus the HSH may be relatively quiescent for the next year or two. As the solar cycle progresses, CMEs and the associated transient flows in the solar wind will become more frequent; interaction regions will merge to form MIRs, which are often preceded by shocks. When these shocks and MIRs arrive at the TS, they push it outward as they propagate through the TS into the HSH. These shocks might produce an increase in the HSH speed, density, temperature, and magnetic field at V1 and V2. In situ observations of the plasma and magnetic fields in the HSH are needed to determine the validity of these expectations.

Shocks and MIRs (including GMIRs) are most numerous near and just after solar maximum. At the last solar maximum near 2001, a series of MIRs with increased density, speed, temperature, dynamic pressure, and magnetic field passed V2 every 6-9 months [Richardson et al., 2003]. The speed at which these shocks move through the HSH is not certain. At Earth, gas dynamic models predict that IP shocks which cross the bow shock maintain the same propagation speed in the magnetosheath as in the solar wind. The increased fast mode speed in the hotter, denser, higher-field sheath region compensates for the reduced flow speed. Szabo et al. [2003, 2004] analyzed IP shock surface normals and propagation speeds in the solar wind and estimated the predicted arrival times in the magnetosheath. They conclude that no systematic deformation is present in the shock pressure front surface. Koval et al. [2005, 2006] model the interaction of IP shocks with the magnetosphere using an MHD model. The MHD model suggests that the speed of the shock front propagation in the magnetosheath decreases from the bow shock toward the magnetopause and the front of the IP shock deforms. Some observations support this prediction; but we note that pickup ions dominate the pressure in the HSH and will affect the shock propagation speeds.

The tilt of the solar magnetic dipole was less than 10° during the solar minima of 1987 and 1996 [Wilcox Solar Observatory]. The latitudinal extent of the HCS was also small, much less than the V1 and V2 heliolatitudes, so we expect that the Voyagers could remain in a unipolar magnetic field region for many months near solar minimum. The V1 magnetic field observations in Figure 12 suggest that the HCS began to move below the latitude of V1 on DOY 135, 2006 [Burlaga et al., 2007a]. Continued observations will determine whether V1 did in fact enter the unipolar region associated with flows from the northern polar coronal hole.

Near solar minimum, the solar wind has large heliolatitudinal speed and density gradients. At the last solar minimum in 1996, V2 was at heliolatitude 16°S and saw a peak speed of 570 km/s, indicating that V2 did not enter the fast coronal hole flow but remained in the transition region between slow and fast solar wind. This result was consistent with estimates that the half-width of the slow wind region was about 15° in 1996 [Richardson and Paularena, 1997] that the width of the boundary layer of a coronal hole flow at 2.5 solar solar radii was 5.4° ± 4.5° [Burlaga et al., 1978]. In the current solar minimum, V2 will be at 28°S and could enter the high-speed solar wind flow. In October 2007, when the tilt of the HCS was about 29°, Ulysses stopped observing low speed solar wind when it moved to heliolatitudes greater than 40°, suggesting a half-width of the slow solar wind region of 11°. If the latitudinal extent of the HCS decreases to the values of the previous two solar cycles, then both Voyagers would be immersed in unipolar regions in the HSH whose origin is the polar coronal holes. The HSH flow would then be relatively fast and its density relatively low, mirroring the upstream conditions. The thermal plasma upstream of a high-latitude shock should have a much higher Mach number, so the temperature in the HSH may be higher. If V2 observes fast flows in the HSH from polar coronal holes, we will learn how these different solar wind conditions affect the plasma and particle heating at the shock. The transition from low to high-speed flow could also drive a large CIR and shock. A shock and speed increase in the solar wind from the crossing of a polar coronal hole boundary were observed at V2 in 2003 [Burlaga et al., 2005a]; similar shocks and speed increases could be observed in the HSH.

## 3.5 Turbulence, Fluctuations and Small-Scale Structure in the Heliosheath

Turbulence and other fluctuations in the HSH might be driven by a number of processes including magnetic reconnection, anisotropic particle distributions, plasma processes associated with the heliospheric current sheet, and the enhancement of solar wind turbulence as it crosses the TS. Observations of a possible reconnection event by V1 do not show enhanced turbulence [Burlaga et al., 2006a, 2007a]. Similarly, crossings of the HCS by V1 are not associated with enhancements in turbulence [Burlaga et al., 2005b, 2006a, 2007b]. Anisotropic particle pressures, which can be produced as particles cross the TS, might lead to "mirror-mode" instabilities [Gary, 1992; McKean et al., 1992; Liu et al., 2007] that could be important for understanding observations of magnetic holes and humps in the HSH [Burlaga et al., 2006b, 2007] (Figure 13). These features could also be produced by solitons; predictions from the theory of soliton waves [Avinash and Zank, 2007] are similar to the observations.

As in the solar wind, the fluctuations of B in the HSH have a multifractal structure and the increments in B have a q-Gaussian (Tsallis) distribution. The increments of B are defined as $dB_n$ = B(t + $2^n$) - B(t), where t is time (in this case in days). Then $dB_0$ = B(t + 1) - B(t) where t refers to successive days. The multifractal structure is observed on scales from 2-16 days in the HSH. The intermittency exponent is a factor of 3.4 smaller in the HSH than in the distant supersonic solar wind [Burlaga et al., 2007a]. The q-Gaussian distribution of increments in B at a scale of 1 day in the HSH during 2006-2007 is broader than that in the distant solar wind, partly because B is larger in the HSH, but the entropic index is the same, q = 1.5±0.04, in both regions (Figure 14). It is not clear why the distribution of B is a Gaussian while the distribution of the increments of B is a q- Gaussian in the HSH. This result might indicate a relationship between the central limit theorem and the generalized central limit theorem in the context of non-extensive statistical mechanics, a topic under investigation in that field.

Figure 15 shows that the shock itself can drive large-scale turbulence in the HSH. It shows the downstream magnetic field strength for a high-Alfven-Mach, strong, supernova shock based on the simulations of Giacalone and Jokipii [2007]. The density fluctuations in the pre-shocked medium distort and ripple the shock, leading to vortical plasma motions in the downstream region that stretch and force together magnetic fields that are frozen into the flow. The fields can be quite large in some places, and quite weak in others. Such processes may be relevant to our understanding of magnetic

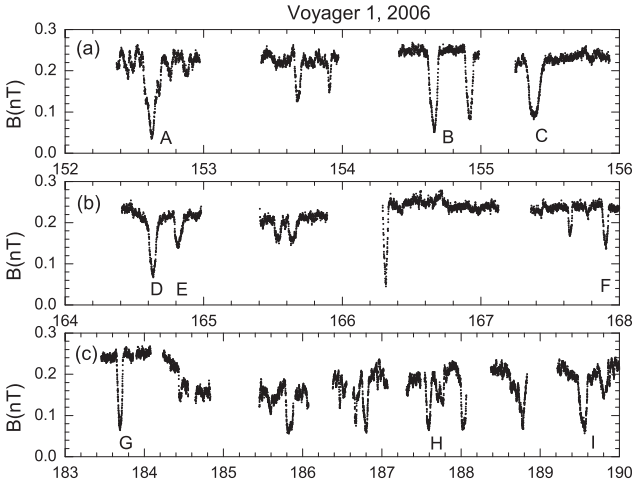


**FIGURE 13.** Magnetic holes in the profile of the magnetic field strength in a unipolar region of the HSH.

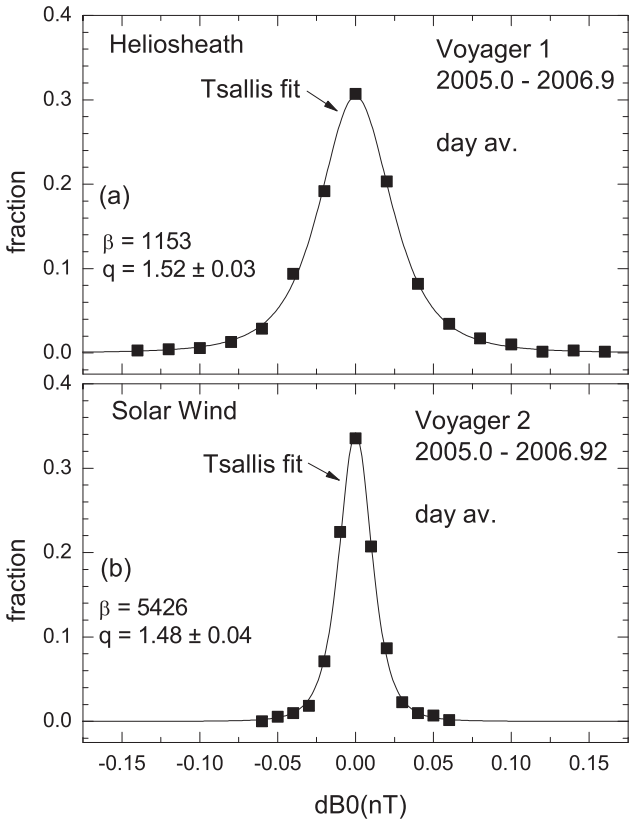


**FIGURE 14.** The distribution of increments of daily averages of B in the HSH (a) and the distant supersonic solar wind (b). Both distributions are described by a Tsallis (q-Gaussian) distribution function with entropic index q = 1.5, shown by the solid curves, but the distribution is wider in the HSH where <B> is stronger.

fields and plasma in the HSH, since the TS is a high-Alfven Mach shock (note that the presence of pickup ions only reduces the sonic Mach number). Burlaga et

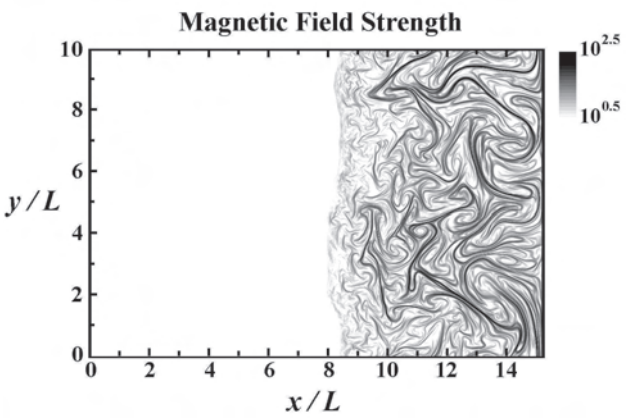


**FIGURE 15.** Contours of the magnetic field strength in the vertical flow behind a shock disturbed by upstream fluctuations in density [Giacalone and Jokipii, 2007]. L is the turbulence coherence length, x is along the shock normal, and y is orthogonal to x.

al. [2007c] suggest that similar enhancements in density (associated with depressions in B, magnetic holes) might be related to the boundaries of vortex cells in compressible turbulence more generally, independent of the generation mechanism. Both observations and models are needed to evaluate the merit of this hypothesis.

### 3.6 IBEX and Voyager: A global picture of the heliosphere

The Interstellar Boundary Explorer (IBEX) is scheduled for launch in the summer of 2008. This NASA Small Explorer mission [McComas et al., 2007] will carry two energetic neutral atom (ENA) single-pixel telescopes mounted transverse to the Sun-oriented spin axis. They will sweep out the entire sky every 6 months, producing line-of-sight-integrated images in energetic hydrogen atoms produced through charge exchange between energetic protons and cold ($<10^4$ K) interstellar hydrogen atoms. IBEX will thereby form all-sky images of the proton populations in the heliosheath beyond the heliospheric termination shock in the energy range 100 eV- 6 keV. This suprathermal proton population is generated by a seed population heated at the termination shock and then likely further accelerated by compressive processes throughout the heliosheath [Fisk and Gloeckler, 2007]. The Voyager 2 plasma measurements just beyond the termination shock have demonstrated that the thermal core proton distribution contains only a small portion of the energy of the upstream solar wind [Richardson et al., 2008], while the partial pressure of 28 keV-17 MeV protons exceeds the magnetic pressure component ($B^2/8\pi$) in the heliosheath [Decker et al., 2008]. Thus the suprathermal proton population in the heliosheath characterizes this huge new plasma regime that is unlike any that we have previously encountered.

Consequently, the 100eV-6keV protons that will be imaged by IBEX are a new population that depends completely on the details of the pickup proton population in the upstream solar wind and on the heating processes at the termination shock (including the foreshock region from which shock-accelerated protons re-enter the termination shock) and throughout the heliosheath. In addition, the Compton-Getting effect severely modifies the intensities of the heliosheath protons that produce the ENAs, so the flow pattern throughout the heliosheath must be understood in order to properly interpret the IBEX ENA images. Without the Voyager 1/2 termination shock crossings, as well as the foreshock and heliosheath observations, the proper interpretation of the IBEX ENA images would have been difficult to attain. The deeper into the heliosheath the Voyagers obtain in situ measurements, the better IBEX will be able to deduce the global structure of the heliosheath from its novel population of suprathermal protons.

### 3.7 Future work

- Study the evolution of the HSH over a solar cycle. Look for evidence that the Voyagers are in HSH flow which began as fast solar wind from coronal holes.
- Look for evidence of transient events in the HSH and link these events to those observed by other spacecraft in the heliospheric network.
- Study small scale structures such as mirror mode waves and possible reconnection sites using both plasma and magnetic field data.
- Combine data from both spacecraft to determine the extent and structure of the heliospheric current sheet in the HSH.
- Study the effect of a tilted HCS on the HSH flows.

## 4. ANOMALOUS COSMIC RAYS AND ACCELERATION

### Anomalous Cosmic Rays

Prior to the V1 TS encounter in late 2004, the prevailing view was that ACRs were accelerated at the TS by diffusive shock acceleration (DSA) to energies ∼1-300 MeV/nuc [Jokipii and Giacalone, 1998; Cummings and Stone, 1998]. However, Figure 16 shows that when V1 crossed the shock at 94 AU on 2004/351, the energy spectrum of ACR He above 10 MeV/nuc did not

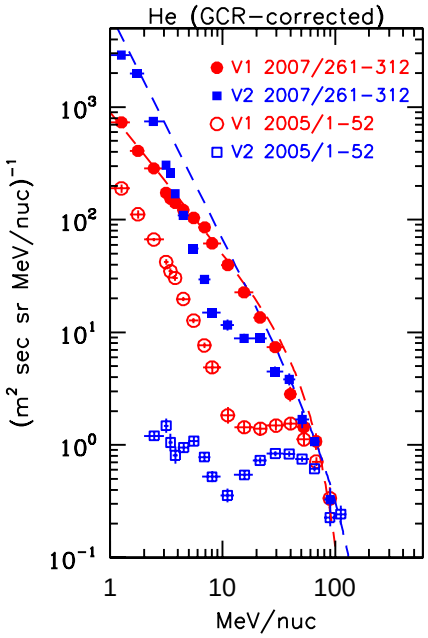


**FIGURE 16.** He spectra corrected for contributions from GCRs for V1 and V2 just after the V1 TS crossing on 2004/351 (open symbols) and just after the V2 TS crossings during 2007/242-243 (filled symbols). Possible source spectra expected at the times of TS crossings are shown as dashed lines (blue appropriate for V2 for r=2 shock and red appropriate for V1 for r=3 shock).

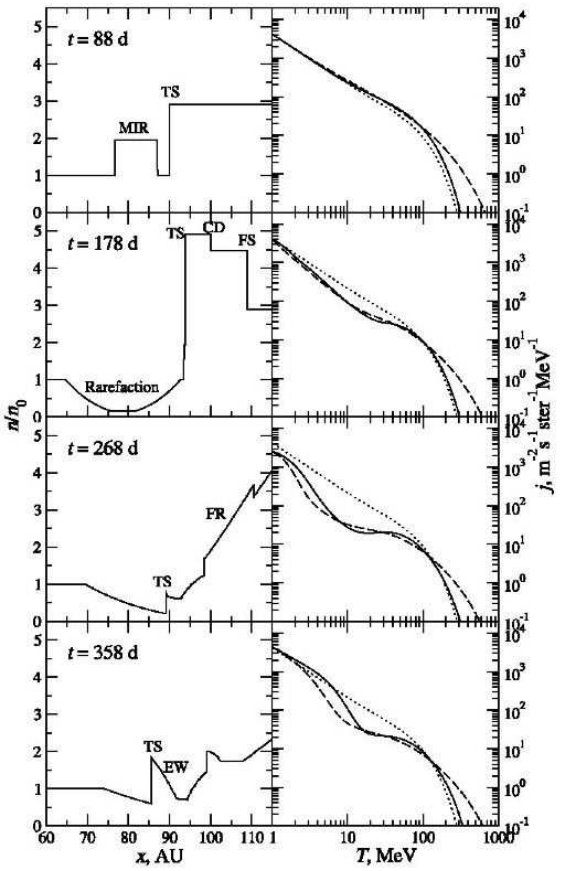


**FIGURE 17.** Temporal evolution of the plasma density (left) and particle spectra (right) at the TS resulting from an incident MIR. Solid and dashed lines refer to different spatial diffusion coefficient models. The pre-MIR spectrum is shown with dotted lines for comparison. (From Figure 3 of Florinski and Zank [2006].)

unroll to the expected source shape, a power-law at lower energies with a roll off at higher energies. After 2004, both the V1 He spectrum in the HSH and the V2 spectrum upstream of the TS continued to evolve toward the expected source shape. The He spectra at V1 and V2 just after V2 crossed the shock are also shown in Figure 16. Between the two crossings, the V2 intensity at 20 MeV/nuc increased by a factor of ∼13 and the V1 intensity increased by a factor of ∼10. Much of these increases must be temporal due to a relaxation of modulation conditions between the source of the ACRs and the spacecraft.

After the V1 TS crossing, several models emerged to explain the deficit of ACRs at mid-energies. Following the finding that the TS motion was inward as V1 crossed it, Jokipii [2006] pointed out that a shock in motion on time scales of the acceleration time of the ACRs, days to months, would cause the spectrum to differ from the expected DSA shape. Florinski and Zank [2006] also provide an explanation based on a dynamic TS. They calculate the effect of MIRs interacting with the TS on the ACR spectral shape. Figure 17 shows that a prolonged period of depressed intensities is produced at mid-energies from a single MIR. A succession of MIRs, as was observed at V2 from 2001 to 2004, presumably could keep the intensities depressed for a long period of time [Cummings and Stone, 2007].

McComas and Schwadron [2006] suggested that at a blunt shock the acceleration site for higher energy ACRs would be at the flanks of the TS, where the injection efficiency would be higher for DSA and connection times of the magnetic field lines to the shock would be longer, allowing acceleration to higher energies. This scenario is shown in Figure 18. Kóta [2007] recently carried out a 2D numerical calculation with an offset spherical TS to simulate the blunt TS and found that, for the parameters chosen, the higher energy ACRs are accelerated mostly in the tail region of the shock.

Fisk et al. [2006] suggest that stochastic acceleration in the turbulent HSH continues to accelerate ACRs and that the high-energy source region would thus be beyond the TS. Several workers have recently included stochastic acceleration, as well as other ef-

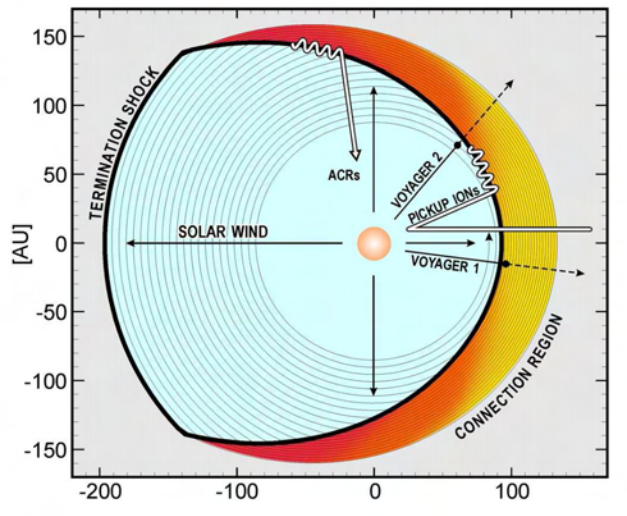


**FIGURE 18.** Schematic diagram of an equatorial cut through the TS. The magnetic field lines in the connection region of the HSH directly connect to the TS source. The approximate positions of Voyager 1 and 2 are shown neglecting their different latitudes. A field line first connects to the TS at the nose. As indicated by the color, the intensity on the field line increases with time as the field line connection points move to the flanks. The ACRs then diffuse along the field line toward the nose of the HSH. (From McComas and Schwadron [2006]).

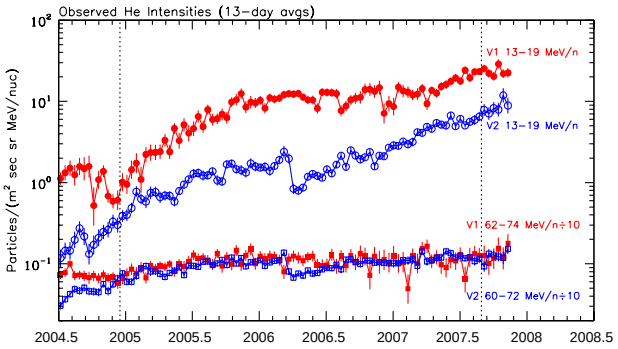


**FIGURE 19.** Intensity of He at V1 and V2 in two energy bands. The V1 and V2 TS crossings are shown as the vertical dotted lines. Note the positive radial gradient at 13-19 MeV/nuc in the HSH after the V2 TS crossing at 2007.66.

fects, in their models [Moraal et al., 2006; Zhang, 2006; Langner and Potgieter, 2006; Ferreira et al., 2007].

Several of these models have produced spectra and time plots that can be compared with the data. Now that V2 has crossed the shock, it is clear that these models require some adjustment. For example, with respect to the model with transient MIRs disturbing the shock, Figure 19 shows that the trend of the V2 13-19 MeV/nuc He intensity indicates that a transient MIR did not cause the modulated shape of the V2 spectrum at the time of its TS crossing. When both spacecraft are in the HSH in late 2007, the radial gradient in the 13-19 MeV/nuc ions does not appear to be caused by a transient. The ∼61-73 MeV/nuc ions have no gradient, so no N-S or longitudinal asymmetry is observed in the ACR intensities at the higher energies.

The other models will have to take into account the long-term temporal variations that were observed. For example, Figure 20 is from Figure 3 of Schwadron et al. [2007], with the addition of a V2 proton spectrum at the time of its crossing. While the model reasonably reproduces the V1 proton spectrum near the TS ($\phi = -5°$ spectrum, where $\phi$ is the longitudinal angle from the nose of the heliosphere), it does not agree with the V2 spectrum, which should be compared to the $\phi = -40°$ spectrum. Also, this model uses a mean free path that is independent of rigidity, and as shown by Cummings and Stone [2007], the spectral scaling between ACR H, $He^+$, and $O^+$ implies a mean free path with a significant rigidity dependence in the rigidity range ∼170 MV to ∼2700 MV. The effect this rigidity dependence has on the energy dependence of the calculated spectra needs to be investigated.

Ferreira et al. [2007] show that a combination of diffusive shock acceleration, adiabatic heating, and stochastic acceleration can approximately reproduce the V1 $He^+$ spectra at the time of the TS crossing, as well as at 100 AU, as shown in Figure 21. Stochastic acceleration was key to the agreement with V1. However, as shown by the right hand panel of Figure 21, the model will require further elaboration to also fit the $He^+$ spectrum at the V2 TS crossing.

In Figure 22, we show the calculated [Ferreira et al., 2007] and observed radial intensity profiles for $He^+$ at ∼20 MeV/nuc from 90 AU to 104.5 AU. After the V1 TS crossing, the observed intensity rose more rapidly than the model predicts, as a result of a strong temporal variation at both V1 and V2 at that time (see Figure 19). However, after ∼96 AU, the gradients predicted by the model are not too different from the V1 observations.

In the next few years, we will continue to observe the evolution of the ACR spectra at both V1 and V2 as a means to discriminate among the different models for the ACR source. It will be interesting to see if the ACR He spectrum unfolds to the 120 AU form shown in Figure 23 over the next few years. The ACR observations will also allow a more definitive determination of the composition of ACRs and of their propagation mean free path in the HS. Heretofore, these determinations have been made upstream of the TS. In the case of composition, the prior studies [Cummings et al., 2002; Cummings and Stone, 2007] relied

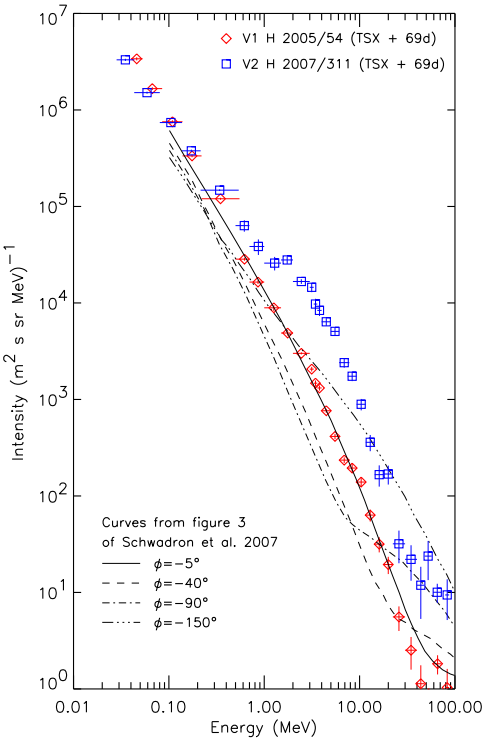


**FIGURE 20.** Differential energy spectrum of protons diffusively accelerated as they move along the TS away from the nose as calculated by Schwadron et al. [2007] using a mean free path parallel to the field, $\lambda_0 = 3$ AU, $\kappa_\perp/\kappa_\parallel = 0.03$, and at a latitude of 35°N. The different curves show the energy spectrum at progressively larger angles from the nose of the shock.

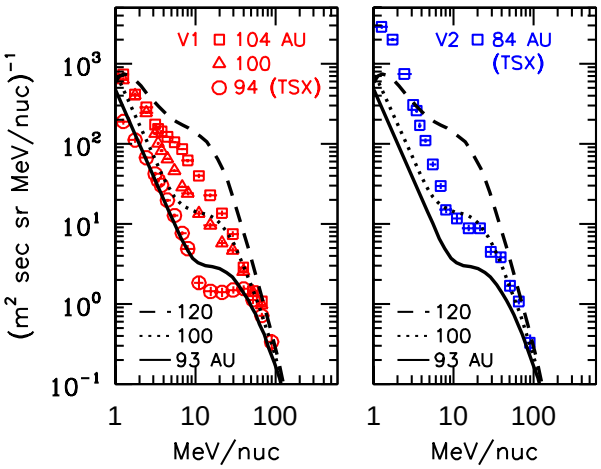


**FIGURE 21.** (left) Computed spectra for singly ionized anomalous He at the TS (93 AU) combining DSA, heating in the inner HSH, and acceleration of a stochastic nature. The observed Voyager 1 spectra (52-day averages) corrected for GCR contributions are also shown. (right) Same as left except V2 observations from 2007/261-312 are shown. (Based on Figure 4 of Ferreira et al. [2007]).

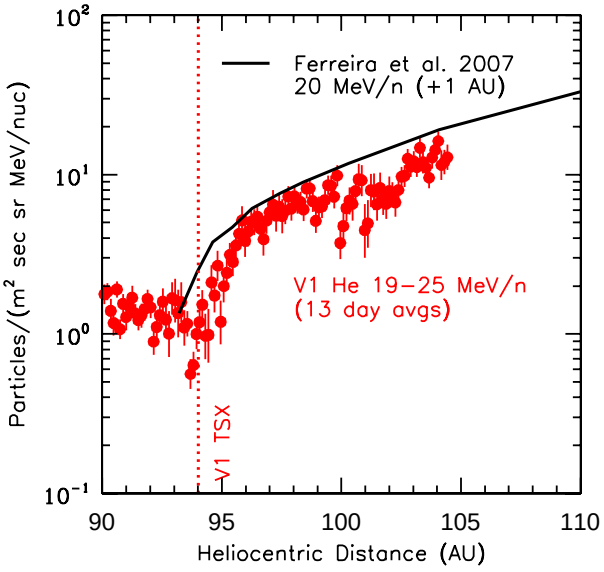


**FIGURE 22.** Computed He radial intensity profile at 20 MeV/nuc along the V1 trajectory using the same acceleration processes as used in Figure 23. The symbols are 13-day averaged V1 18.7-24.7 MeV/nuc intensities. 1 AU has been added to the curve to move the TS from 93 AU in their model to 94 AU as observed. Note the approximate agreement between the gradient of the calculated profile and the observations after ∼96 AU.

on propagation models to extrapolate the high energy measurements down to the power-law portion of the source spectra. In the next few years, we should have an opportunity to observe the source spectra directly.

## Acceleration

An essential aspect of ACR acceleration, particularly by DSA at the TS, is injection. As interstellar neutral atoms are continuously ionized and picked up by the solar wind, their initial velocity-space ring distributions are isotropized to shell distributions, cooled adiabatically to roughly uniform spherical distributions, and evidently also accelerated (adding a sparse halo to the spherical distributions) as they convect outward toward the TS. Thus, pickup ion velocity distributions, f(v) vs. v, that are incident on the TS are expected to have (in the TS frame) a nearly flat "core" component in $0 \leq v \sim 2V_{solarwind}$ plus a falling "tail" component whose form and upper extent depend upon the process that produced them. The relatively high-energy extents of the pickup ion velocity distributions enable them to be injected more easily into the DSA process at the TS. That is, unlike the thermal solar wind, pickup ions arrive at the shock already pre-accelerated. Stochastic processes operate over long periods of time as pickup ions convect with the solar wind

and typically produce exponential tails with e-folding speeds that are sensitive to scattering coefficients and particle species [leRoux and Ptuskin, 1995; Chalov, 2006]. However, Fisk and Gloeckler [2006] point out that a more "robust" statistical process can explain the ubiquitous presence in the inner heliosphere of pickup ion tails with power-law form $f(v) \sim v^{-5}$ [or $j(E) \sim E^{-1.5}$]. Fisk et al. [2006] propagated such a pickup proton distribution to 94 AU, and showed when the $f(v) \sim v^{-5}$ tail passes through the TS, it behaves like an ideal gas, resulting in a downstream pickup proton tail with its intensity increased but its spectral form maintained. Fisk et al. [2006] emphasized that not only could this explain the $j(E) \sim E^{-1.5}$ spectrum of ions 0.04 to ∼2 MeV observed in the HSH [Decker et al., 2005], but, as noted earlier, if the process extends to progressively higher energies further into the HSH, it could also be the acceleration mechanism for ACRs.

### Future Tasks

• Determine the spatial and temporal evolution of the ACR energy spectra of H, He, N, Ne, and O in the HSH and compare with models for the ACR source.
• Compare ACR spectra to estimate the rigidity dependence of the mean free path in the HSH.
• Use measurements of the ACR spectra in the HSH to determine the composition of ACRs.
• Measure particle spectra beyond the HP.
• Compare ACR spectra at V1 and V2 to study global transport, acceleration, and temporal changes.

## 5. GALACTIC COSMIC RAY MODULATION BEYOND THE HELIOSPHERIC TERMINATION SHOCK AND THE INTERSTELLAR COSMIC RAY SPECTRUM

The passage of V2 through the TS in late August of 2007 ushered in a new realm for the study of galactic cosmic rays and the effects of solar modulation. V2 is essentially at the TS and V1 is ∼15 AU beyond it, 30-50% of the way through the HSH to the HP. In 2008 solar activity is near its minimum, so the GCR intensity is at its maximum. In the ensuing 2-3 years, before the solar activity increase in the new cycle is observed in the outer heliosphere, both Voyagers will have journeyed deeper into the HSH. Thus we can study a whole new unexplored region of solar modulation beyond the TS not under the influence of the outward flowing solar wind with the resultant adiabatic energy loss. The interpretation of the observed gradients and time variations will depend strongly on the extension of present modulation models to reflect the newly discovered plasma and magnetic field data beyond the TS.

The ultimate goal is the determination of the interstellar cosmic ray spectra for all species, the primaries such as H, He, C, O, Fe, secondaries such as B and N, and, perhaps most interesting of all, electrons. The spectra, charge and isotopic composition of these different species, all of which the CRS experiment can accurately measure, contain a wealth of information about conditions locally and on a larger scale in the galaxy itself. The plasma density, magnetic field, and the structure and turbulence on large and small scales that determine the actual propagation (diffusion) of these particles throughout the galaxy will be accessible to measure. In this sense Voyager now has already become a true interstellar probe, able for the first time to study astrophysical features of the galaxy that have been previously inaccessible to direct measurement.

This statement is particularly true for electrons. These particles, through their synchrotron radiation in the galactic magnetic fields, are responsible for the galactic radio emission observed from ∼1 to >1000 MHz. This spectrum of radio emission maps out the interstellar electron spectrum which is expected to match that observed by Voyager as it approaches the HP. This process of matching the derived and measured spectra and determining what is necessary to make a match will be an important new area of study that crosses between solar physics modulation and galactic astrophysics propagation. The details of the observations of cosmic rays beyond the TS are changing rapidly but, as of a few months after the V2 TS crossings, several points stand out. Except for lower energy electrons, the intensities of galactic H and He nuclei change little at the TS. Figure 23 shows that the intensities of 265 MeV/nuc GCR He nuclei at V1 and V2 indicate that radial gradients are small, $0.2 \pm 0.2$ %/AU, in the HSH. The overall solar modulation beyond the TS may be small, in contrast to earlier arguments based on data from inside the TS which suggested a potentially large modulation in the outer HSH. The expected LISM GCR He intensity shown in Figure 23 is almost twice the value now observed at V1. This observation implies that significant changes in the previously derived interstellar spectra of cosmic ray nuclei and in the conditions governing cosmic ray propagation in the galaxy may be required.

With the continuing flow of cosmic ray data from the Voyagers in the HSH and the previous 36 years of data from Pioneer, Voyager, Ulysses, IMP, and ACE, we now have a comprehensive record of the spatial and cyclic variations of galactic cosmic rays in the heliosphere. These data provide the basis for more precise modeling of the modulation process which is needed to understand ACE and BESS isotope data and to deter-

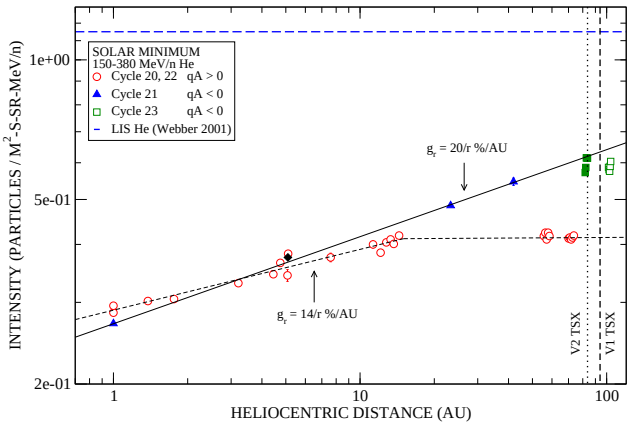


**FIGURE 23.** Solar minimum intensity of 265 MeV/n GCR Helium. The red open circles are from cycles 20 and 22 (qA>0 epoch) when GCR ions drift from the polar regions down to the heliospheric neutral current sheet. The blue triangles and the green squares are from cycles 21 and 23, respectively, when the drift pattern is reversed. All data except V1 and V2 in 2007 are from near the plane of the ecliptic.

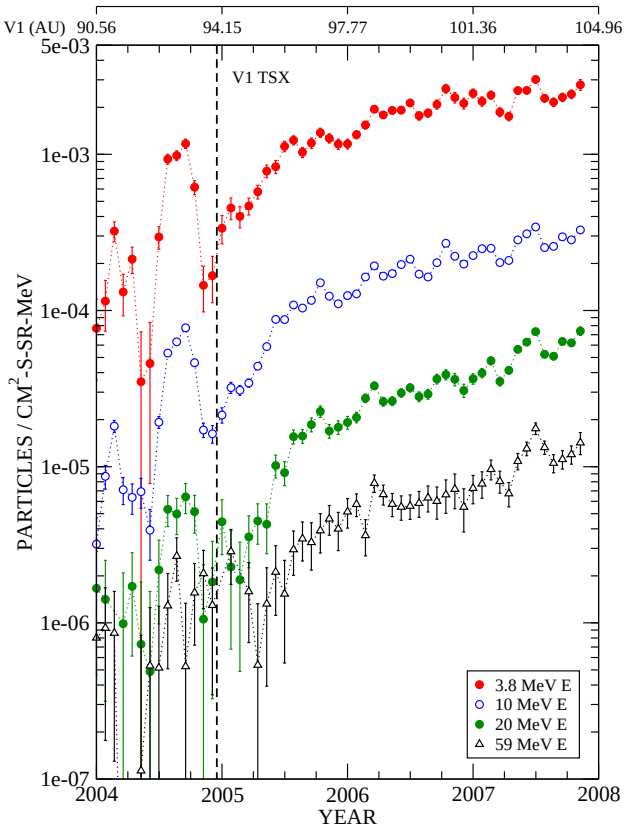


**FIGURE 24.** Background corrected electron time history for five of the seven Voyager electron channels (26-day average) from 2004.0-2007.9. The large intensity increase in the lower channels just before the TS crossing is associated with the passage of the large MIR produced by the 2003 Halloween events.

mine which solar effects produce the long term changes observed in the $^{10}$Be ice core data.

Low-energy electrons are an important astrophysical quantity. However, below 75 MeV they cannot be reliably observed at 1 AU because of large modulation effects and the presence of Jovian electrons. Beginning in 2002.5, large increases in the V1 2.5 - 26 MeV electron intensities coincided with the onset of the first TSP event. These sporadic increases continued over the next 2.4 years and are believed to be related to the interaction of the TS and large MIRs. About 31 days before the TS crossing, the V1 ACR >5 MeV/nuc ions and GCR ion and electron intensities were low. All these populations show a rapid increase in intensity that is temporal in nature and which levels off at about 2005.7. The steady increase in the 3.8-59 MeV electron intensity shown in Figure 24 may be a combination of spatial and temporal effects. If it were spatial in nature, the radial intensity gradient would be ∼18%/AU. Large temporal variations in the 6-14 MeV interval may be related to the passage of transients. Figure 25 shows the energy spectra has a slope of -1.65 and is a factor of ∼100 below the LISM spectra estimated by Langer et. al. [2001]. A large increase in 2.4-26 MeV electron intensities at V2 near day 195, 47 days before the TS crossing, was associated with a strong increase in the magnetic field (see Figure 6).

### 5.1 Future Tasks

• The modulation studies will focus on GCR H and He and their variations relative to ACRs, on GCR electrons, and on observing the onset of cycle 24 in the HSH. These studies will include actively working with the modulation modeling community.

• The Voyager CRS experiment has excellent charge (to Z=28) and isotopic resolution that have been thoroughly analyzed over the solar minimum periods of cycle 22 and 23. We will resume these studies with special emphasis on C, Fe, and $^{10}$B. It should be possible to see the relative changes in the low-energy C and Fe spectra produced by the effects of interstellar ionization energy loss and there is always the possibility of a new low energy component.

• Observe the GCR spectra in the LISM beyond the HP.

## 6. THE HELIOPAUSE AND BEYOND

As shown in Figure 26, the asymmetric forces on the plasma caused by the very local ISMF are believed

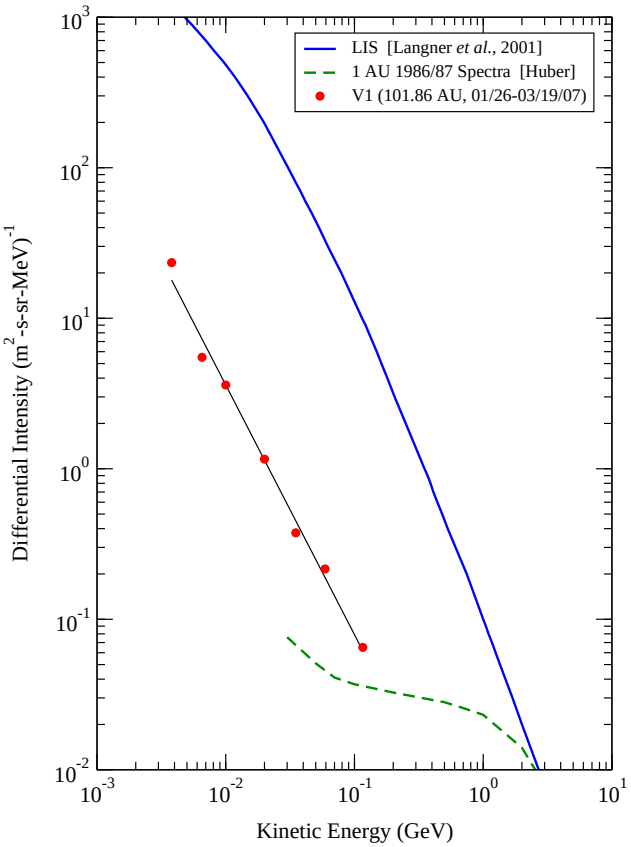


**FIGURE 25.** Electron energy spectra from 2007. The slope is -1.65.

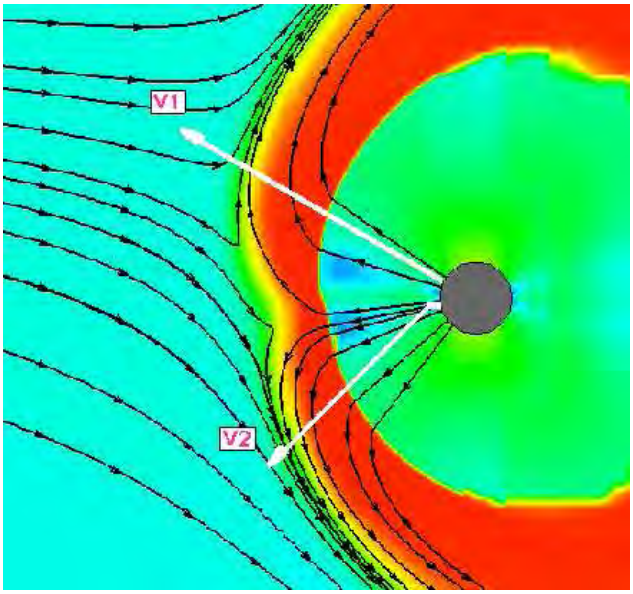


**FIGURE 26.** A current MHD model of the heliosphere showing solar and interstellar plasma flow lines and temperatures [see Opher et al. 2006]. The heliosheath plasma temperature (red) is $\sim 10^6$ K, much hotter than the solar wind (green) or the interstellar wind (blue). The solar plasma flow is deflected tailward in the heliosheath as it approaches contact with the interstellar wind at the heliopause. The model interstellar magnetic field is parallel to the H deflection plane and makes an angle of 45° to the direction of the upstream interstellar wind. The observed heliosheath temperature is only $\sim 10^5$ K, indicating the importance of including pickup ions in heliospheric models.

to cause a asymmetry of the heliosphere. This asymmetry is predicted by simulations [Pogorelov and Matsuda, 1998; Ratkiewicz et al., 1998; Opher et al., 2006, 2007] and is supported by observations [Lallement et al., 2005; Gurnett et al., 2006]. Observations from the Voyagers over the next several years will address key scientific issues of this global interaction.

## 6.1 In Situ Observations and The Large-Scale Structure of the Heliosheath and Heliopause

Now that both Voyagers have crossed the TS and are in the HSH, the next boundary to be sought is the HP. Unlike the case in the solar wind upstream of the TS, the HSH flow is subsonic and the plasma flow speed and magnetic field in the HSH will be affected by the location and nature of the HP. Measurements of the plasma, the magnetic field, the energetic particles, the cosmic rays and the radio emissions will help us understand the nature of the interaction of the heliosphere with the LISM. Once the HP is crossed, the Voyagers will make the first in situ observations of the interstellar medium, adding immeasurably to our understanding of the interstellar medium and the nature of our galaxy. The neutral component of the LISM plays an important role in this interaction, even though it cannot be directly measured.

We believe that the basic physics of the interaction are understood in outline. We expect that the flows of plasma and magnetic field can be approximated described by the magnetohydrodynamic flow equations. But these equations must be augmented by the complicated effects of neutral particles which undergo ionizing processes which then affect the plasma. The effects of energetic particles are not well understood. Simulations, though necessary, cannot yet provide definite predictions of what will be observed. The scientific program must involve the interplay of observations and theory/modeling.

The size and shape of the heliosphere depend on the properties of both the solar wind and the LISM. Among the several physical quantities that describe the interaction of the solar system with the LISM, the least known are the direction and intensity of the ISMF. Models suggest that the strength of ISMF is

a few microgauss. Frisch [1990] analyzed the polarization of light from nearby stars and suggested that these data show the ISMF is parallel to the galactic plane (GAL). Voyager 3kHz radio emission data also show preferred source locations in a plane parallel to the galactic plane [Kurth and Gurnett, 2003]. Lallement et al. [2005] map the solar Lyman-$\alpha$ radiation that is resonantly backscattered by interstellar hydrogen atoms and find that the neutral hydrogen flow direction differs from the helium flow direction by 4°. The H deflection plane (HDP) is tilted from the ecliptic plane by ∼60° and is consistent with an interstellar magnetic field parallel to the HDP plane. However, Pogorelov et al. [2006] suggested that the H deflection does not precisely determine the plane of the magnetic field.

The interstellar magnetic field is frozen into interstellar plasma that is deflected around the HP, causing the field to drape over the HP. If the plane of the interstellar magnetic field were not in the meridional plane of the sun and the angle between the ISMF and interstellar velocity were non-zero, magnetic forces would break the symmetry of the heliosphere. These magnetic forces would cause a distortion of the HP and the TS. For magnetic field intensities of a few microgauss, the ambient interstellar magnetic stresses are comparable to the gas pressure. Opher et al. [2006, 2007] and Pogorelov et al. [2007] suggest that the orientation of the local ISMF affects the streaming direction of ions and neutrals near the TS and Opher thinks it effects the location of heliospheric radio emissions at the HP as well. These studies suggest that the local magnetic field orientation differs from that of the larger scale ISMF, which is thought to parallel the galactic plane.

The major HSH signatures the approaching HP should be a deflection of the plasma flow and an increase in the plasma density. As discussed above, V1 observed the plasma flow rotate as it moved through the HSH toward the HP. Voyager 2 has a functioning plasma detector and is moving in a different direction, so it will provide data complementary to V1. V2 is already observing significant deflections in the HSH flow.

Similarly, in situ observations of the magnetic field from both V1 and V2 should provide additional information concerning the flow patterns and the location of the HP, although the large fluctuations in the magnetic field may mask some of these effects. We expect that the magnetic field magnitude will increase significantly when the Voyagers cross the HP, since the ISMF should be significantly larger than the extended interplanetary magnetic field at the HP.

In analogy with planetary magnetopauses, the HP is likely to be a complex surface that varies locally in thickness and orientation and is the site of processes such as patchy reconnection and a variety of plasma instabilities. Possible reconnection at the HP-LISM interface could accelerate low-energy ions (and electrons), in which case we might observe unusually large departures from the relatively flat, featureless intensities and convection-dominated anisotropies currently observed in the LECP low-energy ion data in the HSH. Intermittent reconnection along a slightly corrugated HP surface might appear in the low-energy ion (and possibly electron) intensity-time profiles as gradual intensity increases with superposed, anisotropic intensity spikes as the spacecraft approaches the HP, similar to the structures encountered in front of the TS. These comments are speculative, drawing largely upon analogies to planetary magnetopauses; however, as with the TS, energetic particle observations will likely enable us to remotely sense the HP well before we cross it. In addition to these processes, some simulations have suggested that various fluid instabilities may be present, which would produce flow signatures and may cause a spreading out of the interface.

## 6.2 Radio Emissions

For over twenty-five years the plasma wave instruments on the two Voyager spacecraft have detected sporadic radio emissions from the outer heliosphere in the frequency range from about 2 to 3 kHz. The source of these emissions is not well understood, although the observed radio emission frequencies (2 to 3 kHz) could only be produced at or near the HP. Shocks have been hypothesized to produce radio emission via energetic electron acceleration at the shock; Kurth and Gurnett [2003] show that the source of these emissions form a line and that the radio emissions were produced when interplanetary shocks interacted with a boundary in the outer region of the heliosphere. Recently, Gurnett et al. [2006] developed a model that the source line is perpendicular to the projection of the ISMF onto the HP. This model is based on the fact that electron acceleration at an interplanetary shock is highly sensitive to the magnetic field direction and is strongest when the magnetic field is nearly perpendicular to the shock normal.

## 6.3 Future Tasks

- Monitor heliospheric radio emissions to try to understand the source of these waves and what they can tell us about the LISM magnetic field direction.
- Use the observations of flow directions in the HSH combined with models to determine the HP location and shape.
- Make the first in situ observations of the LISM.

## 7. SUMMARY

The Voyager spacecraft continue their epic journey of discovery, traveling through a vast unknown region of our heliosphere on their way to the interstellar medium. V2 has just crossed the TS and provided many scientific surprises. Both Voyagers are now traversing the HSH, with the first crossings of the HP and the first in situ observations of the interstellar medium still to come. These encounters could answer many basic, long-standing questions about the plasma and magnetic properties of the LISM, the nature of the TS and its role in the acceleration of the ACRs, the role of the HSH in GCR modulation, the spectra of low-energy interstellar GCRs, and the source and location of the heliospheric radio emissions.

Exploratory missions such as Voyager provide key tests of physical theories and also provide observational surprises which often lead to major advances in physical understanding. The energetic particle beams observed upstream of the TS are certainly an example of such a surprise which has revised current thinking on the morphology of the TS surface. The continued ACR modulation in the HSH, the pre-shock slowdown and lack of heating of the thermal plasma at the TS, the low shock strength of the TS, and increases in the 6-14 MeV galactic electron intensities in the HSH are other examples forcing revisions to long-term hypotheses on particle acceleration. But we have learned to expect surprises from the Voyagers - more are awaited!

The longevity of the Voyagers makes them ideal platforms for studying long-term solar wind and now HSH variations. Their distance make them ideal for studying the evolution of the solar wind, shocks, and cosmic rays. The interpretation of Voyager data is greatly enhanced by the ability to compare with data from Earth-orbiting spacecraft (Wind, ACE, SAMPEX, STEREO), Ulysses, and in the near-future IBEX. These data make deconvolution of solar cycle, distance, and latitude effects possible. To further this intercomparison of data sets and to provide opportunity for the community to provide new insight into these observations, we strongly endorse Guest Investigator and Theory programs focusing on the outer heliosphere. Theory and multi-spacecraft comparisons are needed to provide the best understanding of the data Voyager provides.

## 8. REFERENCES


Avanish, K and G. P. Zank, Geophys. Res. Lett, 34, 5, L05106, 2007.

Baranov, V. B., and Y. G. Malama, J. Geophys. Res., 98, 15157, 1993.

Burlaga et al., J. Geophys. Res., 83, 5167. 1978.

Burlaga, L. F., N. F. Ness, J. W. Belcher, A. Szabo, P.A. Isenberg, and M. A. Lee, J. Geophys. Res., 99, 21511, 1994.

Burlaga, L.F., N.F. Ness, C. Wang, J.D. Richardson, F.B. McDonald, and E.C. Stone, Astrophys. J., 618, 1074, 2005.

Burlaga, L.F., N.F. Ness, M.H. Acuna, R.P. Lepping, J.E.P. Connerney, E.C. Stone, F.B. McDonald, Science, 309, 2027, 2005.

Burlaga L. F., N. F. Ness, and M. H. Acuna, J. Geophys. Res., 111 (A9): A09112, 2006a.

Burlaga L. F., N. F. Ness, and M. H. Acuna, Geophys. Res. Lett., 33 (21): L21106, 2006b.

Burlaga L. F., N. F., Ness, and M. H. Acuna, Astrophys. J. 668 (2): 1246-1258, 2007a.

Burlaga, L. F., A. Vinas, and C. Wang, J. Geophys. Res., 112 (A7), 2007b.

Burlaga L. F., N. F., Ness, and M. H. Acuna, J. Geophys. Res., 112 (A7): A07106 2007c.

Chalov, S., ISSI Scientific Report No. 5, 245, 2006.

Cummings, A.C., and E.C. Stone, Space Sci. Rev., 83, 51, 1998.

Cummings, A.C., E.C. Stone, and C.D. Steenberg, Astrophys. J., 578, 194-210, 2002.

Cummings, A.C., and E.C. Stone, Space Sci. Rev., 130, 389-399, 2007.

Cummings, A.C., and E.C. Stone, 30th Internat. Cosmic Ray, Conf., 2007 (in press).

Decker, R. B., et al., Science, 309, 2020, 2005.

Decker, R.B., E.C. Roelof, S.M. Krimigis, and M.E. Hill, 5th Annual IGPP International Astrophysics Conference. AIP Conference Proceedings 858, Physics of the Inner Heliosheath, 73, 2006.

Decker, R.B., S. M. Krimigis, E. C. Roelof, and M. E. Hill, CP 932, 197, 2007a.

Decker, R.B., S.M. Krimigis, E.C.Roelof, and M.E Hill, Eos Trans. AGU, 88(52), Fall Meet. Suppl., Abstract SH11A-05, 2007b.

Decker, R. B., S. M. Krimigis, E. C. Roelof, M. E. Hill, G. Gloeckler, Armstrong, T. P., Hamilton, D. C., and Lanzerotti, L. J., Science, submitted January, 2008.

Ferreira, S.E.S., M.S. Potgieter, and K. Scherer, J. Geophys. Res., 112, A11101, 2007.

Fisk, L.A., and G. Gloeckler, Astrophys. J. Lett., 640, L79 , 2006.

Fisk, L.A., G. Gloeckler, and T. H. Zurbuchen, Astrophys. J., 644, 631, 2006.

Fisk, L. A., and G. Gloeckler, Space Sci. Rev., 130, 153-160, 2007.

Florinski, V., and G.P. Zank, Geophys. Res. Lett., 33, L15110, 2006

Frisch, P. C., Physics of Outer Heliosphere; Proceedings of the 1st COSPAR Colloquium, Pergamon Press, 19 (1990).

Gary, S.P., J. Geophys. Res., 97, 8519, 1992.

Giacalone, J., Astrophys. J., 625, L37, 2005.

Giacalone, J., and J.R. Jokipii, Astrophys. J., 649, L137, 2006.

Giacalone, J. and J. R. Jokipii, Astrophys. J., 663, L41, 2007.

Gloeckler, G. and L.A. Fisk, Astrophys. J., 648, L63, 2006.

Gloeckler, G., E. Mobius, J. Geiss, M. Bzovski, S. Chalov, S., Astron. Astrophys., 426, 845, 2004.

Gurnett, D.A., and W.S. Kurth, Science, 309, 2025, 2005.

Gurnett, D.A., W. S. Kurth, I. H. Cairns, and J. Mitchell, 5th Annual IGPP International Astrophysics Conference. AIP Conference Proceedings, 858, 129, 2006.

Heerikhuisen, J., V. Florinski, and G. Zank, J. Geophys. Res., 111, A06110, 2006a.

Heerikhuisen, J., N. Pogorelov, V. Florinski, and G. Zank, in American Institute of Physics Conf. Proc. 858, Physics of the Inner Heliosheath: Voyager Observations, Theory, and Future Prospects, ed. J. Heerikhuisen et al. (New York: AIP), 263, 2006b

Heerikhuisen, J., N. Pogorelov, G. Zank, and V. Florinski, Astrophys. J., 655, L53, 2007.

Izmodenov, V., D. Alexashov, and A. Myasnikov, Astron. Astrophys., 437, L35, 2005.

Jokipii, J.R., and J. Giacalone, Space Sci. Rev., 83, 123, 1998.

Jokipii, J.R., J. Giacalone, and J. Kota, Astrophys. J., 611, L141, 2004.

Jokipii, J.R., Science, 307, 1424, 2005.

Jokipii, J.R., 5th Annual IGPP International Astrophysics Conference. AIP Conference Proceedings 858, Physics of the Inner Heliosheath, 143, 2006.

Jokipii, J.R., J. Giacalone, and R.B. Decker, Eos Trans. AGU, 88(52), Fall Meet. Suppl., Abstract SH11A-07, 2007.

Kallenbach, R., A. Czechowski, M. Hilchenbach, and P. Wurtz, in Physics of the Heliospheric Boundaries, ISSI Scientific Report No. 5, 203, 2006.

Kóta, J., and J. R. Jokipii, 5th Annual IGPP International Astrophysics Conference. AIP Conference Proceedings 858, Physics of the Inner Heliosheath, 171, 2006.

Kóta, J., 30th Internat. Cosmic Ray, Conf., 2007 (in press).

Koval, A., J. Safrankova, Z. Nemecek, L. Prech, A. A. Samsonov, and J. D. Richardson, Geophys. Res. Lett., 32, L15101, 2005.

Koval A., J. Safrankova, Z. Nemecek, A. A. Samsonov, L. Prech, J. D. Richardson, M. Hayosh, Geophys. Res. Lett., 33, L11102, 2006.

Krimigis, S.M., R.B. Decker, M.E. Hill, T.P. Armstrong, G. Gloeckler, D.C. Hamilton, L.J. Lanzerotti, and E.C. Roelof, Nature, 426, 45, 2003.

Krimigis, S. M., R. B. Decker, E. C. Roelof, and M. E. Hill, Proc. of the Solar Wind 11/SOHO 16, Connecting Sun and Heliosphere? Conf. (ESA SP-592), p. 21, 2005.

Kurth, W. S., D. A. Gurnett, J. Geophys. Res. 108, 8027, 2003.

Lallement, R., E. Quemerais, J. L. Bertaux, S. Ferron, D. Koutroumpa, and R. Pellinen, Science, 307, 1447, 2005.

Langner, U.W., and M.S. Potgieter, 5th Annual IGPP International Astrophysics Conference. AIP Conference Proceedings 858, Physics of the Inner Heliosheath, 233, 2006.

le Roux, J.A., and V.S. Ptuskin, J. Geophys. Res., 103, 4799, 1998.

le Roux, J.A., G. P. Zank, G. Li, and G. M. Webb, Astrophys. J., 626, 1116, 2005.

le Roux, J.A., G.M. Webb, V. Florinski, and G.P. Zank, Astrophys. J., 662, 350, 2007.

Linde, T. J., T. I. Gombosi, P. L. Roe, K. G. Powell, and D. L. DeZeeuw, J. Geophys. Res., 103, 1889, 1998.

Lipatov, A.S., and G.P. Zank, Phys. Rev. Lett., 82, 3609, 1999.

Liu, Y., J. D. Richardson, J. W. Belcher, and J. C. Kasper, Astrophys. J., 659, L65, 2007.

McComas, D.J., and N.A. Schwadron, Geophys. Res. Lett., 33, L04102, 2006.

McComas, D.J., et al., in Physics of the Inner Heliosheath: Voyager Observations, Theory, and Future Prospects; 5th Annual IGPP International Astrophysics Conference. AIP Conference Proceedings, 858, 241-250, 2006.

McDonald, F.B., E.C. Stone, A.C. Cummings, B. Heikkila, N. Lal, and W.R. Webber, Nature, 426, 48, 2003.

McKean, M. E., D. Winske, and S. P. Gary, J. Geophys. Res., 97, 19,421, 1992.

Moraal, H., R.A. Caballero-Lopez, K.G. McCracken, F.B. McDonald, R.A. Mewaldt, V. Ptuskin, and M.E. Wiedenbeck, Cosmic ray energy changes at the Heliosheath, 219, 2006.

Nerney, S. T., S. Suess and E. J. Schmahl, J. Geophys. Res., (ISSN 0148-0227), 100, A3, p. 3463-3471, 1995.

Opher, M., P. C. Liewer, T. I. Gombosi, W. Manchester, D. L. DeZeeuw, I. Sokolov, and G. Toth, Astrophys. J., 591, L61, 2003.

Opher, M., P. C. Liewer, M. Velli, L. Bettarini, T. I. Gombosi, W. Manchester, D. L. DeZeeuw, G. Toth and I. Sokolov, Astrophys. J., 611, 575, 2004.

Opher, M., E.C. Stone, and P. C. Liewer, Astrophys. J., 640, L71, 2006.

Opher, M. E. C. Stone, and T. Gombosi, Science, 316, 875, 2007.

Parker, E., Interplanetary Dynamical Processes, Interscience, 1962.

Pogorelov, N. V., and T. Matsuda, J. Geophys. Res., 103(A1), 237, 1998.

Pogorelov, N. V., G. P. Zank, and T. Ogino, Astrophys. J., 614, 1007, 2004.

Pogorelov, N. V., and G. P. Zank, in ESA SP-592, Proc. Solar Wind 11 / SOHO 16, Connecting Sun and Heliosphere, Whistler, Canada, 12–17 June, 2005, ed. B. Fleck and T. H. Zurbuchen (Noordwijk, ESA), 35. 2005.

Pogorelov, N. V., and G. P. Zank, Astrophys. J., 636, L161, 2006.

Pogorelov, N. V., G. P. Zank, and T. Ogino, Astrophys. J., 644, 1299, 2006.

Pogorelov, N. V., E. C. Stone, V. Florenski, and G. P. Zank, Astrophys. J., 655, L53, 2007a.

Pogorelov, N.V., E.C. Stone, V. Florinski, and G.P. Zank, Astrophys. J., 668, 624, 2007b.

Ratkiewicz, R. et al., Astron. Astrophys. 335, 363, 1998.

Richardson, J. D., and K. I. Paularena, J. Geophys. Res. 101, 19,995-20,002, 1996.

Richardson, J. D., and C. Wang, Geophys. Res. Lett., 26, 561-564, 1999.

Richardson, J. D., C. Wang, and L. F. Burlaga, Geophys. Res. Lett.,30, 2207, 2003.

Richardson, J. D., C. Wang, and M. Zhang, In AIP Conf. Proc. 858, Physics of the Inner Heliosheath: Voyager Observations, Theory, and Future Prospects, ed. J. Heerikhuisen et al. (New York: AIP), 110, 2006.

Richardson, J. D., Y. Liu, and C. Wang, Adv. Space. Res., 10.1016/j.asr.2007.03.069, 2007.

Richardson, J. D., Y. Liu, C. Wang, and D. J. McComas, in press, Astron. Astrophys., 2008.

Richardson, J. D., J. C. Kasper, C. Wang, J. W. Belcher, and A. J. Lazarus, Science, submitted January, 2008.

Schwadron, N.A., M.A. Lee, and D.J. McComas, Astrophys. J., 2007 (in press).

Stone, E.C., Eos Trans. AGU, 85(47), Fall Meet. Suppl., Abstract SH41B-01, 2004.

Stone, E.C., A.C. Cummings, F.B. McDonald, B.C. Heikkila, N. Lal, W.R., Science, 309, 2017, 2005.

Szabo, A., C. W. Smith, and R. M. Skoug, in Solar Wind Ten, edited by M. Velli, R. Bruno, and F. Malara, AIP Conf. Proc., 679, 782 -785, 2003.

Szabo, A., in Multiscale Processes in the Earth's Magnetosphere: From Interball to Cluster, edited by J.-A. Sauvaud and Z. Nemecek , 57-71, Springer, New York, 2004.

Wallis, M. K., Nature, 254, 202, 1975.

Washimi, H. and T. Tanaka, Space Sci. Rev., 78, 85, 1996.

Washimi, H., G. P. Zank, and T. Tanaka, in AIP Conf. Proc 858, Physics of the Inner Heliosheath: Voyager Observations, Theory, Future Prospects, ed. J. Heerikhuisen (Berlin: Springer), 58, 2006.

Washimi, H., G. P Zank, Q. Hu., T. Tanaka, and K. Munakata, Astrophys. J., 670, L139, 2007.

Wood, B. E., H.-R Miller, G. P. Zank, V. V. Izmodenov, and J. L. Linsky, Adv. Space. Res., 2004.

Zank, G. P., Sp. Sci. Rev., 89, 413, 1999.

Zhang, M., 5th Annual IGPP International Astrophysics Conference. AIP Conference Proceedings 858, Physics of the Inner Heliosheath, 226, 2006.

# 9 TECHNICAL/BUDGET

## 9.1 Introduction

Passage through the termination shock by Voyager 1 in December 2004 and by Voyager 2 in August 2007 began the journey through the transition region, the heliosheath, and the race toward interstellar space. These spacecraft may make the first in situ observations of interstellar space within the next ten years.

The Voyager Interstellar Mission (VIM) started in 1990 when the Voyager spacecraft were over twelve years old, having already returned a wealth of scientific information about the giant gaseous planets and the interplanetary medium between Earth and Neptune. The Voyagers are in their 31st years of flight operations.

Voyager 1 is escaping the solar system at a speed of about 3.6 AU/year while Voyager 2 is leaving at about 3.3 AU/year. Power is the limiting lifetime consumable. The two spacecraft have power to continue returning science data beyond the year 2020. It is likely that at least one of the spacecraft could enter interstellar space while adequate power is still available. All other consumables are adequate for continued operations well past 2020.

## 9.2 The Voyager Spacecraft

Voyager spacecraft subsystems and instruments required for the interstellar mission are operating well and are fully capable of supporting the science mission through at least 2020. Although both spacecraft are operating on some redundant hardware, with careful monitoring of spacecraft health, considerable functional flexibility still exists to operate a long duration mission.

The identical Voyager spacecraft (Figure 27) are three-axis stabilized systems that use celestial or gyro referenced attitude control to maintain pointing of the high-gain antennas toward Earth. The prime mission science payload consisted of 10 instruments (11 investigations including radio science). Only five investigator teams are still funded, though data are collected for two additional instruments, the Planetary Radio Astronomy (PRA) instrument and the Ultraviolet Spectrometer (UVS). Active instruments and their status are described in Section 1: Introduction.

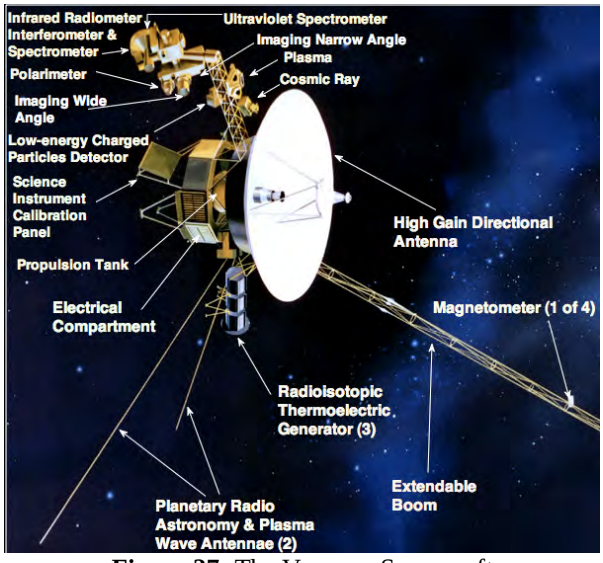


**Figure 27**: The Voyager Spacecraft

The entire Voyager 2 scan platform, including all of the platform instruments, was powered down in 1998. All platform instruments on Voyager 1, except UVS, have been powered down. The Voyager 1 scan platform was scheduled to go off-line in late 2000, but has been left on at the request of the UVS investigator (with the concurrence of the Science Steering Group) to investigate UV emission from the upwind direction. UVS data are still captured, but scans are no longer possible.

| Investigator Teams | **Principal*** and Co-Investigators | |
|---|---|---|
| Plasma Science (PLS) | **J.D. Richardson*** | R. McNutt |
| | J. W. Belcher | E.C. Sittler, Jr. |
| | L.F. Burlaga | C. Wang |
| | A.J. Lazarus | |
| Low-Energy Charged Particles (LECP) | **S.M. Krimigis*** | L.J. Lanzerotti |
| | T.P. Armstrong | B.H. Mauk |
| | R.B. Decker | R. McNutt |
| | G. Gloeckler | E.C. Roelof |
| | D.C. Hamilton | |
| Cosmic Ray Subsystem (CRS) | **E.C. Stone*** | F.B. McDonald |
| | A.C. Cummings | W.R. Webber |
| | N. Lal | |
| Magnetometer (MAG) | **N.F. Ness*** | R.P. Lepping |
| | M. Acuña | C. Smith |
| | L.F. Burlaga | F.M. Neubauer |
| | J.P. Connerney | |
| Plasma Wave | **D.A. Gurnett*** | W.S. Kurth |

Table 1: Voyager Investigations and Status

The Flight Data Subsystem (FDS) and an 8-track digital tape recorder (DTR) provide data handling functions. The FDS configures each instrument. controls instrument operations, collects engineering and science data and formats the data for transmission. The DTR is used to record high-rate PWS data, which are played back about four times per year on Voyager 1. The high rate PWS data on Voyager 2 are no longer useful, so Voyager 2 DTR operations have been terminated to conserve power.

The Computer Command Subsystem (CCS) provides sequencing and control functions. The CCS contains fixed routines, such as command decoding and fault detection, and corrective routines, antenna pointing information, and spacecraft sequencing information. The CCSs on both spacecraft are performing normally.

The Attitude and Articulation Control Subsystem (AACS) controls spacecraft orientation, maintains the pointing of the high gain antenna towards Earth, and controls attitude maneuvers. The AACS circuitry was switched in 2002 and since then the redundant celestial sensors have been used. Following the switch, the new Canopus Star Tracker (CST) lost sensitivity at a higher rate than expected, but since December 2007 the rate of degradation has leveled off. The CST has no problem maintaining lock on the reference star or reacquiring the reference star after maneuvers.

Uplink communication is via S-band (16-bits/sec command rate) while an X-band transmitter provides downlink telemetry at 160 bits/sec normally and 1.4 kbps for playback of high-rate plasma wave data. Receiver 1 on Voyager 2 failed in 1978. Failure of the Tracking Loop Capacitor in Receiver 2 resulted in a drastic reduction in the acquisition frequency bandwidth, requiring the routine use of special procedures to determine the best lock frequency. Voyager 2 is currently operating on the alternate transmitter following an autonomous switch in 1998. The project has elected to remain on the currently selected transmitter. Telecommunications with both spacecraft are normal and the link margins are sufficient to maintain two-way contact with the spacecraft well after 2020.

Electrical power is supplied by three Radioisotope Thermoelectric Generators (RTGs) which are performing nominally. The current power levels are about 286 watts, with power margins of about 34 watts and an average degradation rate of about 4.3 watts per year. As the electrical power decreases, power loads on the spacecraft will have to be turned off, reducing spacecraft capabilities and operational flexibility. Power margins are adequate to operate a complement of science instruments until after 2020.

Spacecraft attitude is maintained by small hydrazine thrusters. One thruster has failed on Voyager 1 (Roll) and one on Voyager 2 (Pitch/Yaw). Additionally, the Pitch/Yaw thruster on Voyager 1 has shown signs of significant degradation, due to exceeding expected end-of-life usage. The thrusters currently in use are expected to last the rest of any mission projection. Nearly 1/3 of the original propellant remains available.

In late 2006, while performing an AACS test, uncommanded power relays were executed onboard Voyager 2. As a result, the magnetometer flippers were activated and the IRIS instrument was commanded on. Commands to return to spacecraft to the correct configuration were sent to the spacecraft and executed properly. A similar uncommanded execution of spacecraft systems occurred in 1998 when the scan platform on Voyager 2 was powered down. The flight team has isolated the probable circumstances that would cause this anomaly and have modified procedures and fault protection algorithms and is generating contingency plans to mitigate possible future occurrences.

The PRA instruments on both spacecraft are being turned off to conserve power. Power and thermal analyses indicated that turning off PRA is safe and the PI has veri-

fied that the data are no longer useful. Voyager 1 turnoff occurred on 15 January 2008. Voyager 2 turnoff has not yet been scheduled.

### 9.3 Operations Concept

The VIM is characterized by (1) science requirements that can be satisfied with observations that are primarily repetitive in nature, and (2) long (and increasing) communication distances. The resulting long round-trip-light-times and decreasing signal levels significantly constrain spacecraft monitoring and control.

Programmatic changes since the beginning of the VIM have significantly reduced flight team staffing levels. As opposed to the multiple teams of specialists
available earlier in the mission, each member of the current flight team performs multiple interdisciplinary functions and only limited backup capability exists.

These mission characteristics and the small team size have resulted in the evolution off the methods used to conduct mission operations. Multi-mission ground data systems are used, though Voyager requires some unique components to maintain compatibility with the multi-mission environment. Dramatic changes have been made to the process for real-time monitoring of routine spacecraft operations. Each of these is discussed further in the following sections.

The mission impact of the reduced staffing includes reduced operational flexibility, greatly reduced anomaly response capability, and potential delays in science data delivery. In addition, many important but non-critical tasks are not being performed.

### 9.4 Sequence Generation

The key to acquiring the desired science observations and maintaining an adequate level of mission adaptivity is the sequencing strategy. Because of the limited flight team resources available for spacecraft sequence generation, this strategy minimizes the labor required while satisfying the science data acquisition requirements and flight system health and safety engineering needs.

Voyager's process of command sequence generation, review and uplink is unique to this mission. It requires continual support by Voyager-experienced personnel.

The sequencing strategy is composed of four basic elements. First is a continuously executing sequence of repetitive science observations and engineering calibrations called the "baseline sequence." A baseline sequence is stored on-board each spacecraft and contains the instructions needed to acquire and return the basic science data to the ground. This sequence will continue to execute for the duration of the mission, but requires periodic adjustment to deal with changes in spacecraft health and configuration, ground system capabilities and the heliospheric environment.

The second element is the storage on-board each spacecraft of the pointing information necessary to keep the boresight of the High Gain Antenna (HGA) pointed at the Earth. This provides the capability for continuous communication with each spacecraft without further HGA pointing commands. HGA Pointing Tables will require updating on both spacecraft within the next few years to maintain the pointing accuracy needed for quality science data acquisition. Special skills are needed for this task, as discussed below.

The third element provides the capability of augmenting the baseline sequence with non-repetitive science or engineering events using either an "overlay sequence," or a "mini-sequence." The difference between these two types of augmentation sequences is that the overlay sequence operates for a fixed interval of time, currently 3 months, and contains all of the baseline sequence augmentations for that time interval. A mini-sequence is focused on accomplishing a single augmentation need and is not a regularly scheduled activity but is done on an as-needed basis.

The fourth element is the use of pre-defined and validated blocks of commands (high level sequencing language), rather than the optimized sequence of individual commands (low level sequencing language) used during the prime mission, to accomplish desired spacecraft functions. The use of pre-defined blocks of commands greatly reduces the effort required to generate and validate a sequence of commands. The spacecraft contains pre-defined blocks of commands to support this functionality for routine activities.

### 9.5 Transmitting the Data to the Ground

The Voyager Interstellar Mission is, with one exception, a real-time data acquisition and return mission. All of the operating instruments on each spacecraft are continuously collecting data for immediate transmission to Earth. The normal real-time transmission data rate is 160 bits per second (bps), including 10 bps engineering data

The one exception to real time data return is that once a week, 48 seconds of high rate (115.2 kbps) plasma wave data are recorded onto the DTR on Voyager 1. Currently, a second 48 seconds per week is recorded on Voyager 1. The high rate data are no longer usable on Voyager 2. These data are played back about every 6 months and provide increased spectral resolution snapshots of the plasma wave information. These high rate plasma wave data provide the primary data for the Plasma Wave Investigation Team's estimate of the termination shock and heliopause locations. Recording and playback of Voyager 1 high rate plasma wave data can continue until 2010 when telecommunications capability will no longer support the playback data rate of 1.4 kbps.

### 9.6 Capturing the Data on the Ground

Real-time telemetry data capture is accomplished using 34- and 70-meter tracking antennas of the DSN. Capture of the recorded high rate plasma wave data from Voyager 1 requires the use of an array of 70- and 34-meter antennas.

Twelve hours per day of tracking support for each spacecraft is the project's target for science data acquisition. But because Voyager is usually allocated support

after higher priority mission requirements have been satisfied, the recent average daily support has averaged 8-10 hours. Future increases in missions being supported by the DSN will result in reduced tracking station availability for the Voyagers. As tracking support is reduced, the ability to characterize the heliospheric medium is degraded. Acceptable minimum science data acquisition requirements range from 4 to 8 hours per day per spacecraft, depending on the specific investigation.

### 9.7 Delivery to Science Investigation Teams

Science data are provided electronically to the science investigation teams in the form of a Quick Look Experiment Data Record (QEDR) and Experiment Data Record (EDR). Voyager 1 and Voyager 2 QEDRs for each science investigation are generated daily (Monday through Friday) containing the available data since the last QEDR was produced. Since these products are produced in near real-time, generally within 24 hours of the data capture, data gaps due to a variety of ground system problems are present in the QEDR. Once a week, EDRs are created for the previous week's data which fille data gaps resulting from ground problems to the extent possible. When the final EDRs are available, science teams are notified by electronic mail. The science teams then retrieve the data at their convenience for further processing and analysis.

### 9.8 Spacecraft Monitor and Control

Spacecraft monitor and control includes the real-time functions necessary to monitor spacecraft health and to transmit and verify commands to insure data capture during special activities and support non-real-time functions. With the reduced flight team staffing during VIM and the acceptability of increased risk during an extended mission, real-time support is limited to weekday prime shift and special off-shift events (commanding, DTR playbacks, and attitude maneuvers). This reduced real-time monitoring support was enabled by the development and implementation by Voyager personnel of an automated telemetry monitoring tool which alerts on-call personnel to potential anomalous spacecraft conditions. This automation tool, Voyager Alarm Monitor Processor Including Remote Examination (VAMPIRE), has served as a model for development of a similar multi-mission tool now in use by other missions.

Maintaining spacecraft health and safety is a non-real-time function. It includes: the analysis of engineering telemetry data to establish and evaluate subsystem performance trends; the periodic in-flight execution and analysis of subsystem calibrations and engineering tests; analysis of AACS, FDS, and CCS memory readouts; the review and updating of telemetry alarm limits; the identification and analysis of anomalous conditions; and the implementation of corrective actions. Detailed anomaly analysis has suffered recently because of the level of staffing.

The analysis of engineering telemetry data to establish and evaluate subsystem performance trends is an important operations function. It drives decisions about future optimum configurations for maximizing mission lifetime. The analysis of these data relies on the system and subsystem expertise retained by the individual flight team members. Like anomaly analysis, as the flight team has lost subsystem expertise due to the retirement of experienced personnel and the downsizing of the flight team, the ability to perform trend analysis has been severely impacted. Though some new tools have been implemented over the last two years, development of an automated process for trend data gathering and display is considered a crucial future development to improve operations efficiency.

Periodic in-flight calibrations and engineering tests are used for verifying spacecraft performance, analyzing anomalies, and maintaining spacecraft capabilities. While some of these calibrations and tests are included in the baseline sequence, the majority are initiated from the ground in either an overlay or mini-sequence.

The identification and analysis of anomalous conditions and the determination of recommended corrective actions relies on the system and subsystem expertise of the individual flight team members. An automated tool, Monitor/Analyzer of Real-time Voyager Engineering Link (MARVEL) monitors CCS/FDS telemetry data to assist the analyst with normal event verification and to display on a workstation screen any conditions that are not as predicted. MARVEL performs limited analysis of the CCS/FDS telemetry and identifies possible causes of the anomalous condition and potential corrective actions from the stored knowledge base within the program.

### 9.9 Protection Against Spacecraft Failures

In order to maximize the spacecraft science data return reliability for a mission that could potentially continue until 2020 or beyond, automated safeguards against possible mission-catastrophic failures are provided.

Each spacecraft has Fault Protection Algorithms (FPAs) stored on-board that are designed to recover the spacecraft from otherwise mission-catastrophic failures. The FPAs are mostly implemented in the CCS although a few are interactive with the AACS. The five FPAs stored in the CCS execute pre-programmed recoveries for the following:

- AACS anomalies
- Loss of command reception capability
- Exciter and transmitter hardware anomalies
- CCS hardware and software anomalies
- Anomalous power loads

In addition, fault correction routines in the AACS deal with failures of its circuits and sensors.

The second safeguard is the Backup Mission Load (BML), which provides automated on-board protection against the permanent loss of command reception capability. Without command reception capability, the spacecraft must continue to operate with the instructions previously stored in the CCS memory. The BML reconfigures the spacecraft for maximum telecommunications and attitude control reliability and modifies the Baseline Load to continue the acquisition and transmission of fields, particles and waves science data as long as the spacecraft continues to function.

All of the above protection mechanisms require periodic review and occasional modifications by the Flight Team. These are dictated by planned configuration changes and by unpredictable changing conditions.

### 9.10 Consumables Management

Both spacecraft have on-board consumables that are adequate to support spacecraft operation until at least 2020. Electrical power is the major consumable which limits the spacecraft lifetime. Power should be adequate to support science data acquisition until at least 2020 and possibly beyond. Both spacecraft have about 30 kg of hydrazine that provides about 50 years of operation at current usage rates.

### 9.11 Mission Adaptivity

While Voyager is primarily a non-adaptive real-time data acquisition and return mission, two types of science data acquisition and return adaptivity exist. Both types have been successfully used during VIM.

The first type of adaptivity is the recovery of a high rate PWS playback that is not captured with the initial playback. The response to the loss of a playback is to sequence a second playback prior to the time when data on the DTR is overwritten with newly recorded data. For normal baseline sequence recording of PWS data this allows 6 months to execute a second playback.

The second type of adaptivity is to increase the frequency of high rate PWS recordings and playbacks. This was done in response to increased plasma wave activity during cruise and the predicted Voyager 1 termination shock crossing . An on-board sequence block allows increasing the high rate PWS recordings by sending a single command to the spacecraft. It can record one PWS frame about every nine hours over a period of two weeks or one additional frame per week for six months. The latter mode is in use on Voyager 1 and doubles the resolution of the PWS high-rate data.

### 9.12 Science Management

The Project Scientist coordinates with the Voyager Science Investigators, the science community, and other elements of the Project to ensure that the Project scientific objectives are met. The Science Steering Group (SSG) is chaired by the Project Scientist and consists of the Principal Investigators for the funded investigations (see Table 2). The SSG has the leading role in the overall optimization of the science return from the mission and in the resolution of conflicting science requirements.

Although funding for UVS and PRA has been discontinued by NASA, both these data sets are still being received. The UV data are made available to Jay Holberg at the University of Arizona, and the PRA data to Michael Kaiser at GSFC. As mentioned earlier, the Voyager 1 PRA instruments has been turned off and the Voyager 2 instrument is slated to be turned off in the very near future for power conservation.

The principal investigators are responsible for analyzing their data and reporting their findings in a timely manner. They participate, as appropriate, in making these results available to the science community and to the general public. They present their results at science conferences, through news releases and via publications in the popular press and scientific journals. More than 150 refereed and non-refereed papers have been published since 2005. A list of published papers, by investigation, is available at http://voyager.jpl.nasa.gov/science/bibliography.html

The principal investigators provide archival data to the National Space Science Data Center at Goddard.. Archived data can be accessed via the NSSDC Master Catalog at the following URLs:
http://nssdc.gsfc.nasa.gov/nmc/tmp/1977-084A.html
http://nssdc.gsfc.nasa.gov/nmc/tmp/1977-076A.html

A summary of data availability is accessible at the Sun-Earth Connection Data Availability Catalog at http://spdf.gsfc.nasa.gov/SPD/SPDTopMatrixNASA.pl In addition, a list of URL's, which point to science data, including those at the investigators' home institutions, is located at the JPL Voyager web site at http://voyager.jpl.nasa.gov/.

## 10 EDUCATION AND PUBLIC OUTREACH

Voyagers E/PO plan will support NASA themes "NASA Keeps Me Informed About What's Going On with the Sun", and "The Solar System Is an Astrophysical Laboratory for NASA".

To accomplish this the Voyager Project will continue its 7-year partnership with the NASA/JPL Ambassador Program. Project team members will keep ambassadors informed of Voyager 1's status in the heliosheath and Voyager 2's crossing of the Termination Shock and entrance into the heliosheath. We will continue our participation in Los Angeles's Better Educated Students for Tomorrow (BEST) Project. The Voyager Project will support educator workshops at JPL for the NASA Explorer School program with space science materials and activities where appropriate.

The Voyager Project will assist the Interstellar Boundary Explorer (IBEX) outreach lead in developing a 3D model of the Voyager spacecraft for a new segment to "Time Space" planetarium show at the Adler Planetarium. We will support a variety of education and public outreach resources to be distributed with the planetarium show. As a partnership with the Space Weather Action Center, ACE, and Ulysses missions, Voyager plans to help increase education of the 3D Heliosphere and the Solar Cycle

## 11 BUDGET

Since the beginning of the Voyager Interstellar Mission, the project has continually adapted its operations concept and workforce in response to changes in funding levels. The project has undergone a continual transition from multiple specialized teams to a single operations team wherein each member performs multiple interdisciplinary functions. New, internally developed processes and efficiency enhancements have made this possible.

Similarly, there have reductions in the level of funding for science data processing, analysis and archiving. Even with the slight increase resulting from the 2005 Senior Review, funding only allows for minimal science. The

funding reductions have resulted in a reduction in the number of graduate students and post-docs supported by the project, so the co-investigators are performing much of the data processing and validation.

Of great concern, given the current level of funding is the effect of inflation over the next five years. The relatively flat guidelines will result in an erosion of science funding due to inflation by about 20% over the period 2008-2012 and will result in even further reductions in workforce assigned to process, analyze and archive the science data. The proposed optimum budget would correct for some of the losses caused by inflation.

Since 1998, Voyager has shared project management with the Ulysses project. With Ulysses mission operations terminating in FY2008 and the closeout of science processing, analysis and archiving in FY09, this sharing arrangement will end and Voyager may require augmentation in its project office.

The minimum budget would allow continued operations at the current minimum level, including costs to support the minimum flight team described above and the current low level of project management support. The guideline budget includes costs for science center functions related to operating the instruments and performing quick-look data processing. Also included are limited science analyses required to ensure proper instrument operations and the validity of the data before they are archived. Science data analysis funds allow for limited science analysis and the publication and presentation of select papers, primarily of major science events.

The proposed optimal science budget would permit study of a broader range of science topics and important augmentations in science center data products. Some of the benefits from this increased budget:

- Improve the quality and timeliness of Voyager MAG data sent to the Voyager Investigators, other Scientists, and the NSSDC, and support our analysis and understanding of the MAG data.
- Improve access to detailed CRS documentation to assist other investigators/students in using the data.
- Provide access to CRS data via web services to the SSSC Virtual Observatories.
- Enable more in-depth analysis of science data than that afforded in the guideline budget.
- Provide for more comparisons of solar wind features in the inner and outer heliosphere to understand the solar wind evolution.
- Increase participation of undergraduate and graduate students in data processing and analysis. This would introduce younger scientists into the space physics community.

In 2005 the Flight Team identified more than seventy tasks that would improve the operations infrastructure, replace and reduce the number of old workstations, update software modules and improve productivity and enhance personnel effectiveness. While some progress has been made, much has not been accomplished because of lack of workforce and/or lack of financial resources.

Though we have upgraded most of our operational workstations, many of the software tools currently in use are no longer supported and require that we maintain out of date hardware systems. New technologies now make possible automated tools to reduce workloads and the potential for errors, improve spacecraft health monitoring, and provide for more confident long-range planning.

The optimal budget would provide funds to address the items deemed most important. One-time investments in FY09 include:

- Software modifications required to migrate the data management system to modern computers. This would enhance science data delivery and provide backup capability while reducing the number of workstations required for this task by 67%.
- Development of a temperature estimation tool which would allow the Voyager team to make decisions about optimum and/or safe thermal balance when reconfigurations due to decline in power become necessary
- Update the RTG model to refine long-range power output predictions.

There is also an ongoing need for an increase in personnel as follows:

- An increase in computer system administration support. Current support levels have been insufficient to support changes in the AMMOS software and the infusion of more modern workstations into the Mission Operations area and have resulted in significant workflow inefficiencies for Flight Team members.
- Increase project management to full time beginning in mid FY09

Attributable Deep Space Mission Systems costs, though not part of the Voyager budget submission, are included in Table IV, Line 2a of Appendix 1. These are based on approximately 10 hours of coverage per day per spacecraft, using both the 34-meter and the higher cost 70-meter antenna. Direct Multimission Ground Systems and Services costs are included in Item 2a of Tables I and II.

Voyager is the only mission currently exploring the heliosheath. The spacecraft are capable of continued operations and are in position *now* to characterize interaction of the solar and interstellar winds. Voyager provides unique in situ information about this region of space and, with IBEX, will significantly increase our knowledge about the global area of space at and beyond the termination shock. Both spacecraft are poised to encounter the heliopause and enter interstellar space within the next 10-15 years. Continuation of the mission at the optimal level would allow for a more robust science mission that would answer fundamental questions about the interactions between the solar and interstellar media. Furthermore, it would provide for a more robust and lower risk operations environment and reinstate a small degree of flexibility for development of further enhancements and efficiency improvements to Flight Team processes

# Appendix 1
# List of Acronyms

| Acronym | Meaning |
|---|---|
| $xsxK | Thousands Of Dollars |
| AACS | Attitude & Articulation Control Subsystem |
| ACE | Advanced Composition Explorer |
| ACR | Anomalous Cosmic Ray |
| AMMOS | Advanced Multi-Mission Operations System |
| AU | Astronomical Unit |
| B | Magnetic Flux |
| BS | Bow Shock |
| BEST | Better Educated Students for Tomorrow |
| BML | Backup Mission Load |
| C | Carbon |
| CCS | Computer Command Subsystem |
| CMIR | Corotating Merged Interaction Region |
| CRS | Cosmic Ray Subsystem Experiment |
| DSA | Diffusive Shock Acceleration |
| DOY | Day of Year |
| DSN | Deep Space Network |
| DTR | Digital Tape Recorder |
| EDR | Experiment Data Record |
| ENA | Energetic Neutral Atom |
| E/PO, EPO | Education & Public Outreach |
| eV | Electron volts |
| FDS | Flight Data Subsystem |
| Fe | Iron |
| FPA | Fault Protection Algorithm |
| FTE | Full-Time Equivalent |
| GAL | Galactic Plane |
| GCR | Galactic Cosmic Ray |
| GMIR | Global Merged Interaction Region |
| GSFC | Goddard Space Flight Center |
| H | Hydrogen |
| HCS | Heliospheric Current Sheet |
| HDP | Hydrogen Deflection Plane |
| He | Helium |
| HGA | High-Gain Antenna |
| HP | Heliopause |
| HSH | Heliosheath |
| IBEX | Interstellar Boundary Explorer |
| ICME | Interplanetary Coronal Mass Ejection |
| IMF | Interplanetary Medium |
| IMP | Interplanetary Monitoring Platform |
| IRIS | Infrared Interferometer Spectrometer and Radiometer |
| ISMF | Interstellar Magnetic Field |
| ISM | Interstellar Medium |
| JPL | Jet Propulsion Laboratory |
| K | Kelvin (degrees) |
| KeV | Thousands of Electron Volts |
| kHz | KiloHertz |
| K-12 | Kindergarten through 12$^{th}$ grade |
| LECP | Low-Energy Charged Particles Experiment |
| LISM | Local Interstellar Medium |
| Ly $\alpha$ | Lyman Alpha |
| MAG | Magnetometer Experiment |
| MARVEL | Monitor/Analyzer Of Real-Time Voyager Engineering Link |
| MHD | Magnetohydrodynamics |
| MeV | Million Electron Volts |
| $\mu$G | MicroGauss |
| MIR | Merged Interaction Region |
| NASA | National Aeronautics & Space Administration |
| N | Nitrogen |
| Ne | Neon |
| NSSDC | National Space Science Data Center |
| NSTA | National Science Teachers Association |
| nuc | Nucleon |
| O | Oxygen |
| PLS | Plasma Science Experiment |
| PRA | Planetary Radio Astronomy |
| PUI | Pickup Ions |
| PWS | Plasma Wave Subsystem Experiment |
| QEDR | Quicklook EDR |
| RTG | Radioisotope Thermoelectric Generator |
| SOHO | Solar & Heliospheric Observatory |
| SSSC | Sun-Solar System Connection |
| SSG | Science Steering Group |
| SW | Solar Wind |
| TS | Termination Shock |
| TSP | Termination Shock Particles |
| URL | Uniform Resource Locater |
| UT | Universal Time |
| UVS | Ultra-Violet Spectrometer |
| V | Velocity |
| V1 | Voyager 1 |
| V2 | Voyager 2 |
| VAMPIRE | Voyager Alarm Monitor Processor Including Remote Examination |
| VIM | Voyager Interstellar Mission |